European Journal of Taxonomy 811: 1–50
https://doi.org/10.5852/ejt.2022.811.1725
ISSN 2118-9773
www.europeanjournaloftaxonomy.eu
2022 · Sulakhe S. *et al.*

Monograph

urn:lsid:zoobank.org:pub:4EAB19E4-9B7A-48DC-88ED-C15CE31EC96D

Arboreal gems: resurrection of *Isometrus sankeriensis* Tikader & Bastawade, 1983 and descriptions of two new species of *Isometrus* Ehrenberg, 1828 (Scorpiones: Buthidae) from the Western Ghats, India

Shauri SULAKHE [1,*], Shubhankar DESHPANDE [2], Gaurang GOWANDE [3], Nikhil DANDEKAR [4] & Makarand KETKAR [5]

[1,2,3,4,5] InSearch Environmental Solutions, C-26/9, Ketan Heights, Kothrud, Pune, Maharashtra 411038, India.
[1,5] Institute of Natural History Education and Research (INHER), B1-602, Kumar Parisar, Kothrud, Pune, Maharashtra 411038, India.
[2] Department of Environmental Science, Fergusson College, Pune, Maharashtra 411004, India.
[3] Annasaheb Kulkarni Department of Biodiversity, Abasaheb Garware College, Karve Road, Pune, Maharashtra 411004, India.
[3] Department of Biotechnology, Fergusson College, Pune, Maharashtra 411004, India.

[*] Corresponding author: shaurisulakhe@gmail.com
[2] Email: shubhankarsdeshpande11@gmail.com
[3] Email: gaurang.gowande@gmail.com
[4] Email: conservewithnikhil@gmail.com
[5] Email: makketkar@gmail.com

[1] urn:lsid:zoobank.org:author:F0811269-C3F3-4489-9E77-7E70F2F1E9B8
[2] urn:lsid:zoobank.org:author:80E36A9E-017F-49D4-AC67-77EA63E9F56F
[3] urn:lsid:zoobank.org:author:1D0ED49C-6286-4E7E-AE14-C0EEB9DBBCAF
[4] urn:lsid:zoobank.org:author:3D0B9F18-86CF-4A6D-929E-98249D59ED4A
[5] urn:lsid:zoobank.org:author:DEBFABFA-D8D1-44F4-99AB-7EA1A0DDF2B5

Abstract. The Western Ghats of India is considered one of the richest biodiversity hotspots in the world. Documenting scorpion diversity has always been of paramount importance due to their species richness, ecological role and endemism, which calls for conservation priority. Scorpion diversity of the Western Ghats is probably underestimated given the ancestry of the group, and more field work in the region is very likely to uncover numerous undescribed taxa. Several new Indian species have recently been discovered in the scorpion genus *Isometrus* Ehrenberg, 1828 (Scorpiones: Buthidae). In this communication, we resurrect *I. sankeriensis* Tikader & Bastawade, 1983 and describe two new species from the Western Ghats of India, *I. nakshatra* sp. nov. and *I. wayanadensis* sp. nov., using an integrative taxonomic approach. In order to replace the lost holotype of *I. sankeriensis*, we designate a neotype and reassess the identity of this species. This work elevates the number of species of *Isometrus* found in India to eight and we expect many more scorpion discoveries from India with continued research.

Keywords. COI, 16S, time-dating, species delimitation, cryptic species, phylogenetics.

Sulakhe S., Deshpande S., Gowande G. Dandekar N. & Ketkar M. 2022. Arboreal gems: resurrection of *Isometrus sankeriensis* Tikader & Bastawade, 1983 and descriptions of two new species of *Isometrus* Ehrenberg, 1828 (Scorpiones: Buthidae) from the Western Ghats, India. *European Journal of Taxonomy* 811: 1–50. https://doi.org/10.5852/ejt.2022.811.1725

Introduction

The Western Ghats (WG) is a chain of high mountains along the western coast of India, running from the Tapti River in the north to the southern tip of India near Kanyakumari, with an average elevation of 800 m a.s.l. (Tawde & Singh 2015). Prioritization for conservation has led to the demarcation of 34 biodiversity hotspots in the world, including the WG (Myers *et al.* 2000; Mittermeier *et al.* 2004). Limited biotic exchanges with other regions have resulted in a remarkable local endemism in the WG (Bossuyt *et al.* 2004). Scorpions are an important component of numerous ecosystems (Polis *et al.* 1981; Rafinejad *et al.* 2020). Recent arachnological surveys in India have resulted in the descriptions of many new species of scorpions (Sulakhe *et al.* 2020a, 2020b, 2020c, 2020d, 2020e, 2021; Mirza 2020). Cryptic species are considered problematic in taxonomic studies (Mirza *et al.* 2018), as it is difficult to distinguish them based on morphology alone, leading to taxonomic confusion (Lajmi *et al.* 2016). Prior to the implementation of molecular tools, many species were thought to have wide distributional ranges. However, advanced molecular and statistical techniques are now being combined with traditional taxonomy and are playing a major role in the discovery of new species and also in helping establish appropriate conservation priorities (Chaitanya *et al.* 2019; Mallik *et al.* 2020; Sulakhe *et al.* 2020a; Gowande *et al.* 2021).

The family Buthidae C.L. Koch, 1837, is the largest scorpion family with ca 95 genera and ca 1259 species distributed across the globe (Rein 2021). The genus *Isometrus* Ehrenberg, 1828 previously contained two subgenera, *Isometrus* (*Isometrus*) Ehrenberg, 1829 and *Isometrus* (*Reddyanus*) Vachon, 1972. Tikader & Bastawade (1983) described another subgenus, *Isometrus* (*Closotrichus*), based on the position of trichobothria *db* on the fixed finger of the chela, and with *I.* (*Closotrichus*) *sankeriensis* Tikader & Bastawade, 1983 from Sankeri, Karwar, Karnataka, India as the type species. Tikader & Bastawade (1983) incorrectly placed *I. thurstoni* Pocock, 1983 and *I. maculatus* (DeGeer, 1778) in the subgenus *Reddyanus*, and these were later transferred by Kovařík (1994) to *Isometrus* (*Isometrus*). Kovařík (1994) also synonymized *I.* (*Closotrichus*) with *I.* (*Isometrus*). In his review of the genus *Isometrus*, Kovařík (2003) synonymised *I. sankeriensis* with *I. thurstoni* based on the samples available in his collection, which he considered to be *I. sankeriensis*. Kovařík *et al.* (2016) elevated the subgenus *I.* (*Reddyanus*) to genus level.

The genus *Isometrus* comprises five species found in India, including the type species, *I. maculatus*. Although *I. maculatus* has a vague type locality (ambiguously described as "Suriname and Pennsylvania"), it is assumed that the species originated in South Asia (Fet & Lowe 2000; Lourenço & Huber 2002; Veronika *et al.* 2013; Kovařík *et al.* 2016). The remaining Indian species of this genus include *I. thurstoni* described from Shevaroy Hills (Tamil Nadu), *I. tamhini* Sulakhe *et al.*, 2020 from Tamhini, Pune (Maharashtra), *I. amboli* Sulakhe *et al.*, 2020 from Amboli, Sindhudurg (Maharashtra) and *I. kovariki* Sulakhe *et al.*, 2020 from Chikkadunnasandra, Bengaluru (Karnataka).

Sulakhe *et al.* (2020a) described two new species, *I. tamhini* and *I. amboli*, from the northern Western Ghats (NWG) of India. Sulakhe *et al.* (2020a) were unable to test the conspecificity of these two taxa with *I. sankeriensis* using morphological and molecular data due to the unavailability of material that could objectively be attributed to *I. sankeriensis*. However, based on the analyses of specimens newly collected from the type locality of *I. sankeriensis*, they appear to be morphologically and genetically

Table 1. Morphometric data for *Isometrus sankeriensis* Tikader & Bastawade, 1983. Abbreviations: L = length; W = width (in carapace corresponding to median width); D = depth.

Dimensions (mm)		♂ **neotype** BNHS SC 194	♂ **topotype** INHER 288
Carapace	L/W	3.37/2.74	3.67/3.24
Mesosoma	L	7.99	9.06
Tergite VII	L/W	2.20/2.87	2.20/2.81
Metasoma and telson	L	19.97	22.41
Segment I	L/W	2.52/1.58	2.45/1.57
Segment II	L/W	1.17/1.42	3.03/1.41
Segment III	L/W	3.43/1.38	3.40/1.42
Segment IV	L/W	3.84/1.21	3.66/1.43
Segment V	L/W	4.70/1.17	5.15/1.23
Telson	L/W/D	4.31/1.00/1.13	4.72/1.09/1.21
Pedipalp	L	15.14	16.23
Femur	L/W	4.07/0.89	4.39/0.92
Patella	L/W	4.43/1.11	4.74/1.17
Chela	L	6.64	7.10
Manus	W/D	1.16/0.96	1.22/1.10
Movable finger	L	4.20	4.48
Pectine	L/W	2.48/0.59	2.90/0.68
Genital Operculum	L/W	0.51/0.97	0.58/1.05
Total	**L**	**31.33**	**35.14**
Pectinal teeth count	PTC	15/16	16/18

distinct from *I. thurstoni*, which warrants the removal of this species from synonymy. However, the resurrection of *I. sankeriensis* also directly raises doubts about the validity of the two species described by Sulakhe *et al.* (2020a), given the morphological similarity and geographic proximity in the distribution of these three species.

In this communication, we test the validity of *I. amboli* and *I. tamhini*, as well as that of the putative species occurring throughout the Western Ghats using a hierarchical species delimitation approach across geographical, molecular and morphological axes. We here resurrect *I. sankeriensis* as a valid species and provide a detailed description and diagnosis of it using an integrative taxonomic approach. As the holotype of *I. sankeriensis* is lost, we herein designate a neotype of *I. sankeriensis*, in accordance with the recommendations of Article 75 of the International Code of Zoological Nomenclature (ICZN 2000). As a part of our extensive surveys to study populations of *Isometrus* from the WG of India, we describe two new species using an integrated taxonomic approach.

Material and methods

Sampling (Tables 1–3)

Sampling was carried out in the Western Ghats, India. Specimens were located with the help of ultraviolet light (AmiciVision 18W 100 LED UV Torch), and a few specimens from each locality surveyed were collected. Photographs of the specimens were taken using a Nikon D500 with a 105 mm F2.8 micro lens and R1C1 flash kit. Specimens were euthanized and preserved in absolute ethanol and

Table 2. Morphometric data for *Isometrus nakshatra* sp. nov. Abbreviations: L = length; W = width (in carapace corresponding to median width); D = depth.

Dimensions (mm)		♂ **holotype** BNHS SC 195	♂ **paratype** INHER 275	♀ **paratype** INHER 276	♀ **paratype** BNHS SC 196
Carapace	L/W	5.35/4.58	4.58/4.08	4.44/3.90	5.31/4.48
Mesosoma	L	10.78	9.96	10.34	15.16
Tergite VII	L/W	3.18/4.51	2.75/3.61	2.55/3.85	3.47/5.47
Metasoma and telson	L	30.79	24.41	21.82	28.22
Segment I	L/W	3.50/2.36	0.74/1.98	2.53/2.05	2.81/2.60
Segment II	L/W	4.41/2.11	3.73/1.78	3.13/1.87	3.89/2.35
Segment III	L/W	4.93/2.08	4.00/1.70	3.37/1.72	4.39/2.11
Segment IV	L/W	5.15/2.02	4.45/1.67	3.27/1.61	4.85/1.99
Segment V	L/W	6.73/1.82	5.97/1.63	4.46/1.44	6.06/1.94
Telson	L/W/D	6.07/1.74/1.88	5.52/1.35/1.53	5.06/1.25/1.34	6.22/1.62/1.73
Pedipalp	L	35.72	27.92	18.06	23.5
Femur	L/W	10.80/1.22	8.25/1.03	4.97/1.22	6.50/1.49
Patella	L/W	11.30/1.36	8.74/1.21	5.31/1.53	6.86/1.96
Chela	L	13.62	10.93	7.78	10.14
Manus	W/D	1.29/1.15	1.03/1.03	1.28/1.19	1.63/1.51
Movable finger	L	8.32	6.71	5.50	7.03
Pectine	L/W	3.78/0.89	3.33/0.75	2.77/0.70	3.39/0.89
Genital Operculum	L/W	0.75/1.21	0.62/1.05	0.62/0.94	0.82/1.23
Total	**L**	**46.92**	**38.95**	**36.60**	**48.69**
Pectinal teeth count	PTC	15/15	16/15	15/15	15/15

later transferred to 70% ethyl alcohol in collection jars for long term preservation. Examination and morphological measurements were done using a Leica EZ4HD microscope with the Leica application suite. Morphometry was performed following Stahnke (1970); trichobothrial terminology follows Vachon (1974); metasoma carination follows Francke (1977); pedipalp carination follows Prendini (2016); leg terminology follows Tikader & Bastawade (1983); morphological terminology follows Hjelle (1990); pedipalp chela dentition follows González-Santillán & Prendini (2013); and lateral ocelli terminology follows Loria & Prendini (2014). Measurements were taken (in mm) for 32 morphological characters (Tables 1–3). Specimens collected and studied are deposited in the museum collection of the Bombay Natural History Society (BNHS), Mumbai and the Institute of Natural History Education and Research (INHER), Research Laboratory, Pune, Maharashtra, India. Material from the Zoological Survey of India, Calcutta (ZSI) was also studied.

Comparative material examined

Data used for the comparison, diagnosis and statistical analysis of *I. maculatus*, *I. thurstoni*, *I. tamhini*, *I. amboli* and *I. kovariki* was sourced from Sulakhe *et al.* (2020a, 2020b).

Molecular analysis

DNA extraction, amplification and sequencing

The protocol according to Sulakhe *et al.* (2020a) was followed. Genomic DNA was isolated from preserved (ethanol 99.9%) muscle tissue (leg fragment) of species of *Isometrus* with the help of Macherey-Nagel

Table 3. Morphometric data for *Isometrus wayanadensis* sp. nov. Abbreviations: L = length; W = width (in carapace corresponding to median width); D = depth.

Dimensions (mm)		**holotype** BNHS SC 190	**paratype** INHER 279	**paratype** BNHS SC 193	**paratype** INHER 279	**paratype** INHER 280	**paratype** INHER 281	**paratype** BNHS SC 191	**paratype** BNHS SC 192
Carapace	L/W	4.55/3.98	4.49/4.14	4.32/4.00	4.76/3.99	4.91/4.43	4.76/4.32	4.77/4.26	4.69/4.24
Mesosoma	L	13.71	12.71	10.86	12.16	10.77	13.39	14.09	15.14
Tergite VII	L/W	3.41/4.06	3.35/3.70	3.00/3.32	2.91/4.33	2.72/4.63	3.03/4.86	3.04/4.72	2.97/4.89
Metasoma and telson	L	32.73	30.42	31.20	24.37	27.44	24.57	24.85	25.88
Segment I	L/W	3.49/2.03	3.38/1.96	3.52/1.96	2.32/2.25	3.05/2.23	2.53/2.03	2.48/2.20	2.40/2.27
Segment II	L/W	4.51/1.74	4.33/1.77	4.42/1.80	3.36/2.03	3.76/1.12	3.44/1.84	3.46/2.04	3.67/1.97
Segment III	L/W	4.96/1.70	4.77/1.68	4.87/1.66	3.69/1.96	4.09/1.91	3.69/1.85	3.70/1.89	3.94/1.85
Segment IV	L/W	5.73/1.78	5.45/1.66	5.59/1.55	4.19/1.79	4.60/1.91	4.13/1.82	4.08/1.86	4.56/1.79
Segment V	L/W	7.48/1.67	6.63/1.63	6.71/1.62	5.35/1.73	5.80/1.83	5.28/1.65	5.61/1.72	5.66/1.69
Telson	L/W/D	6.56/1.58/1.79	5.86/1.46/1.63	6.1/1.6/1.7	5.46/1.41/1.57	6.14/1.50/1.60	5.50/1.44/1.56	5.52/1.44/1.48	5.65/1.52/1.57
Pedipalp	L	22.38	21.69	21.97	17.97	19.33	18.47	18.27	18.51
Femur	L/W	6.28/1.20	6.13/1.21	5.80/1.14	4.70/1.29	5.01/1.33	4.71/1.33	4.75/1.33	4.87/1.35
Patella	L/W	6.59/1.57	6.39/1.60	6.66/1.49	5.23/1.72	5.57/1.93	5.23/1.82	5.26/1.75	5.36/1.84
Chela	L	9.51	9.17	9.51	8.04	8.75	8.53	8.26	8.28
Manus	W/D	1.85/1.42	1.83/1.44	1.79/1.46	1.60/1.38	1.83/1.48	1.72/1.44	1.70/1.48	1.78/1.42
Movable finger	L	5.77	5.47	5.58	5.39	5.88	5.77	5.64	5.51
Pectine	L/W	3.47/0.76	3.31/0.72	3.40/0.70	3.05/0.74	3.41/0.78	3.13/0.76	3.12/0.77	3.05/0.77
Genital operculum	L/W	0.88/1.32	0.74/1.13	0.64/1.12	0.67/1.25	0.75/1.31	0.86/1.27	0.75/1.27	0.84/1.31
Total	**L**	**50.99**	**47.62**	**46.38**	**41.29**	**43.12**	**42.72**	**43.71**	**45.71**
Pectial teeth count	PTC	16/16	17/17	17/17	16/16	16/18	15/15	15/15	15/16

Table 4. Voucher numbers and GenBank accession numbers for the sequence data used in the phylogenetic analysis.

	Species	Voucher	GeneBank Accesion Number (*COI*)	References (*COI*)	GeneBank Accesion Number (*16S*)	References (*16S*)	Locality
1	*I. thurstoni*	INHER 130	MT027823	Sulakhe *et al.* 2020a	OK644019	this study	type locality
2	*I. thurstoni*	INHER 141	MT027893	Sulakhe *et al.* 2020a	–	–	type locality
3	*I. thurstoni*	INHER 139	MT027892	Sulakhe *et al.* 2020a	–	–	type locality
4	*I. tamhini*	BNHS SC 155	MT027221	Sulakhe *et al.* 2020a	OK644014	this study	type locality
5	*I. tamhini*	BNHS SC 156	MT027224	Sulakhe *et al.* 2020a	–	–	type locality
6	*I. tamhini*	INHER 73	MT027033	Sulakhe *et al.* 2020a	–	–	type locality
7	*I. tamhini*	INHER 170	MT250512	Sulakhe *et al.* 2020b	–	–	Saltar Khinda, Maharashtra
8	*I. tamhini*	INHER 342	OK641843	this study	OK644013	this study	Bhivegaon, Maharashtra
9	*I. tamhini*	INHER 343	OK641842	this study	–	–	Bhivegaon, Maharashtra
10	*I. amboli*	BNHS SC 157	MT027898	Sulakhe *et al.* 2020a	OK644015	this study	type locality
11	*I. amboli*	BNHS SC 158	MT027894	Sulakhe *et al.* 2020a	–	–	type locality
12	*I. amboli*	INHER 111	MT027891	Sulakhe *et al.* 2020a	–	–	type locality
13	*I. amboli*	INHER 161	MT260056	Sulakhe *et al.* 2020b	–	–	type locality
14	*I. kovariki*	BNHS SC 162	MT260061	Sulakhe *et al.* 2020b	OK644023	this study	type locality
15	*I. kovariki*	INHER 146	MT260065	Sulakhe *et al.* 2020b	–	–	type locality
16	*I. kovariki*	INHER 149	MT260060	Sulakhe *et al.* 2020b	–	–	type locality
17	*I. sankeriensis*	BNHS SC 194	MW136340	this study		–	type locality
18	*I. sankeriensis*	INHER 289	MW463935	this study	OK644018	this study	type locality
19	*I. nakshatra* sp. nov.	INHER 275	MW463941	this study	–	–	type locality
20	*I. nakshatra* sp. nov.	INHER 276	MW463940	this study	OK644020	this study	type locality
21	*I. nakshatra* sp. nov.	INHER 294	OK641848	this study	OK644021	this study	Agumbe, Karnataka
22	*I. nakshatra* sp. nov.	INHER 296	MW463939	this study	–	–	type locality
23	*I. wayanadensis* sp. nov.	BNHS SC 190	MW463936	this study	OK644022	this study	type locality
24	*I. wayanadensis* sp. nov.	BNHS SC 193	MW463938	this study	–	–	K.S. Colony, Karnataka
25	*I. wayanadensis* sp. nov.	INHER 219	MW463937	this study	–	–	type locality
26	*Isometrus sp.*	INHER 41	OK641846	this study	–	–	Dandeli, Karnataka
27	*Isometrus sp.*	INHER 154	OK641845	this study	–	–	Dandeli, Karnataka
28	*Isometrus sp.*	INHER 156	OK641844	this study	OK644016	this study	Anshi, Karnataka
29	*Isometrus sp.*	INHER 157	OK641847	this study	OK644017	this study	Anshi, Karnataka
30	*I. maculatus*	AMCC LP- 1798	KY982207	Esposito *et al.* 2018	KY981921	Esposito *et al.* 2018	Sri Lanka
31	*Lychas mucronatus*	MNHN-JAB19	JN018211	–	–	–	–
32	*Lychas mucronatus*	–	–	–	AF370855	–	–

Table 5. Primers used for PCR amplification and sequencing of COI and 16S mitochondrial genes**.**

Primer: cytochrome c oxidase I	5'–3' primer sequence	Source
HCO2198	TAAACTTCAGGGTGACCAAAAAATCA	Folmer *et al.* 1994
HCOoutout	GTAAATATATGRTGDGCTC	Prendini *et al*. 2003
LCO1490	GGTCAACAAATCATAAAGATATTGG	Folmer *et al.* 1994
Nancy	CCCGGTAAAATTAAAATATAAACTTC	Simon *et al.* 1994
Chelicerate F1	TACTCTACTAATCATAAAGACATTGG	Barrett & Hebert 2005
Chelicerate R1	CCTCCTCCTGAAGGGTCAAAAAATGA	Barrett & Hebert 2005
Chelicerate R2	GGATGGCCAAAAAATCAAAATAAATG	Barrett & Hebert 2005
Primer: 16S rRNA	**5'–3' primer sequence**	**Source**
16Sar	CGCCTGTTTATCAAAAACAT	Simon *et al*. 1994
16Sbr	CTCCGGTTTGAACTCAGATCA	Giribet *et al.* 1996

NucleoSpin® DNA Insect kit following the manufacturer's protocols. Voucher numbers and GenBank accession numbers of specimens generated in this study and used for DNA analysis are provided (Table 4, Figs 1–2) and other sequences were sourced from Sulakhe *et al.* (2020a, 2020b). A 550–600 base pair (bp) fragment of the cytochrome c oxidase subunit I (*COI*) and a 450–500 base pair (bp) fragment of the 16S rRNA (16S) mitochondrial gene were amplified by polymerase chain reaction (PCR) using the primers listed in Table 5. A 25 µl PCR reaction (TaKaRa Taq™ DNA Polymerase) was prepared containing 1 unit of Taq DNA polymerase (0.2 µL), 2.5 µL of 10 × buffer, 2 µl of dNTPs (2.5mM each), 2 µl (5mM) of each primer, 2 µl template DNA and 14.3 µl of water, and reactions were carried out with an Miniamp Thermal Cycler. The thermal cycler profile used for amplification of the COI gene was as follows: 95°C for 3 min (initial denaturation temperature 95°C for 3 min, denaturation temperature 95°mC for 30 s, annealing temperature 55°C for 30 s, elongation temperature 72°C for 45 s and 3 min × 35 cycles.

The thermal cycler profile used for amplification of the 16S gene was as follows: 95°C for 3 min (initial denaturation temperature 95°C for 3 min, denaturation temperature 95°C for 30 s, annealing temperature 52°C for 30 s, elongation temperature 72°C for 45 s and 3 min × 35 cycles. PPCR products were cleaned through column purification with the Qiagen PCR Cleanup Kit and sequenced with a 3730 DNA Analyzer. The sequencing primers were the same as those used in PCRs. All sequences were deposited in the GenBank® nucleotide sequence database (http://www.ncbi.nlm.nih.gov) under the accession numbers given in Table 4.

The sequences were also checked with the BLAST (Altschul *et al.* 1990) tool to find the closest available sequences in GenBank® and related ones were downloaded for analysis.

Sequence alignment

Generated sequences were cleaned manually in MEGA ver. 7 (Kumar *et al.* 2016) using chromatograms visualised in Chromas ver. 2.6.5 (Technelysium PTY. Ltd). Cleaned and downloaded sequences were aligned using MUSCLE (Edgar 2004) implemented in MEGA (Kumar *et al.* 2016) with default parameters. The final *COI* alignment contained 31 sequences, each 525 bp in length, whereas the *16S* alignment contained 12 sequences, each of 500 bp length. Each alignment included one available sequence of *I. maculatus* from Sri Lanka as a part of the ingroup, and one sequence of *Lychas mucronatus* (Fabricus, 1798) was used as the outgroup to root the phylogenetic tree. The *COI* and *16S* datasets were concatenated and the resultant 1025 bp long alignment was used for molecular phylogenetic analyses.

Molecular phylogenetic analyses

Maximum Likelihood (ML) analysis was performed in the web implementation of IQ-tree (Nguyen *et al.* 2015) under the (TN + F + G4: *COI* position 1, TN + F + I: *COI* position 2, HKY + F: *COI* position 3, TPM3 + F + G4: *16S*) models of sequence evolution, determined using ModelFinder (Kalyaanamoorthy *et al.* 2017) on the IQ-tree web platform, and branch support was tested using 1000 non-parametric rapid ultrafast bootstrap pseudo-replicates (Minh *et al.* 2020). The *COI* region was partitioned per codon position, whereas the non-coding *16S* region was not partitioned.

Time-calibrated phylogenies were built in BEAST ver. 1.10.4 (Suchard *et al.* 2018). Since no fossil data exist for the genus *Isometrus* or other closely related buthid genera, a relaxed log-normal molecular clock was used following Loria & Prendini (2020). The concatenated dataset was partitioned as *COI* and *16S* loci, and the molecular clocks and substitution rates were unlinked across the partitions, whereas the trees were linked. A Speciation : Yule prior was implemented for construction of the trees. A review of the literature dealing with divergence time estimations for scorpions revealed that clock rates for the mitochondrial *COI* and *16S* regions have been established for the family Buthidae. Accordingly, a normal clock rate prior was applied to the *COI* and *16S* regions, with the following settings: $\mu = 0.007$, $\sigma = 0.00146$ for *COI* and $\mu = 0.005$, $\sigma = 0.00270$ for *16S*. The models of sequence evolution for each partition were tested using PartitionFinder ver.1.1.1 (Lanfear *et al.* 2012), using a greedy search algorithm. The models suggested were as follows: HKY + I + G for *COI* and HKY + G for *16S*. Bayesian inference (BI) analysis was run for 150 000 000 generations, sampling every 3000 generations. The Effective Sample Size (ESS) values for the analysis were sufficiently higher than 200 for all parameters, and the convergence was tested using Tracer ver. 1.7 (Rambaut *et al*. 2018). A 50% majority rule consensus tree was compiled using TreeAnnotator ver. 1.10.4 with a burn-in of 10%. The tree was visualised and edited in FigTree ver. 1.4.4 (Rambaut 2009).

Species delimitation analysis

We followed a modified version of the hierarchical approach by Shanker *et al.* (2017) towards the delimitation of species within *Isometrus*. Initially, a BI tree with ultrametric output, based on the concatenated dataset, was reconstructed using the method mentioned above to visualize the clustering pattern of the sequences. The tree revealed the presence of a few putative novel lineages within the Western Ghats. Whether these putative lineages qualified as distinct species was tested using PTP, bPTP, GMYC, ABGD, *p*-distance and molecular divergence dating.

A coalescence based species delimiting approach was used to estimate the number of putative species. To this end, we used the Bayesian Poisson Tree Processes (bPTP) model, which considers an evolutionary placement algorithm to estimate the number of Operational Taxonomic Units (OTU) from a phylogenetic BI tree with the ultrametric tree as input (Zhang *et al.* 2013). This model delimits species in terms of number of substitutions based on input from a rooted phylogenetic tree. As bPTP is an updated version of the original maximum likelihood PTP, the maximum likelihood PTP search result is part of the bPTP results. The online server for bPTP was used to run 500 000 MCMC iterations with a thinning parameter of 100 and burn-in of 0.1 to obtain convergence (http://species.h-its.org/ptp/).

Apart from bPTP, we also used another molecular species delimitation approach, the generalized mixed Yule-coalescent (GMYC) method (Fujisawa & Barraclough 2013). GMYC models speciation (among-species branching events) via a pure birth process and within-species branching events as neutral coalescent processes. GMYC identifies the transition points between inter- and intra-species branching rates on a time-calibrated ultrametric tree by maximizing the likelihood score of the model. It assumes that all lineages leading from the root to the transition points are different species (Esselstyn *et al.* 2012).

An online implementation of GMYC (https://species.h-its.org/gmyc/) was used in single threshold mode with the ultrametric tree as input.

Numerous tests show that bPTP outperforms GMYC on simulation data, and bPTP results are comparable to GMYC on real datasets (Zhang *et al.* 2013).

Genetic delimitation of species was also performed using barcode gap analysis in the Automatic Barcode Gap Discovery (ABGD) software (Puillandre *et al.* 2012) using simple distances and a transition of 2.0.

We also calculated the genetic *p*-distance for the mitochondrial loci *COI* and *16S* in MEGA ver. 7. Within Buthidae, recently described species belonging to the genus *Olivierus* Farzanpay, 1987, namely *O. mikhailovi* Fet *et al*., 2021, *O. tarabaevi* Fet *et al*., 2021 and *O. voldemari* Fet *et al*., 2021, are 3.25% to 3.9% divergent from *O. gorelovi* Fet *et al*., 2018 in the *COI* gene. Hence, with *p*-distance, we considered a threshold of 3.25% in *COI* to delimit the species included in our analyses. Based on empirical data we have considered a threshold of 2% in *16S* to delimit the species in our analyses.

We considered putative species that showed strong separation on a minimum of four axes identified by PTP, bPTP, GMYC, ABGD, *p*-distance and time divergence.

In addition to this molecular species delimitation approach, this study is supplemented by morphology to characterise the newly described and resurrected species.

The purpose of estimating the time divergence was to serve as an additional line of evidence in the delimitation of species. A threshold of 3 Mya from The Most Recent Common Ancestor (TMRCA) for sister lineages was considered sufficient to diagnose the species, based on a review of the literature (Loria & Prendini 2020; Fet *et al.* 2021).

Morphological statistical analysis

Since males show stronger morphological differences than females and since we have a better representation of male specimens in our collection, we have chosen to use only males in morphometric analyses. Statistical analysis of the morphometric data was performed on size-adjusted measurements by taking all measurements as a percentage of carapace median length (CML) to remove bias due to body size variation. Multivariate normality of the data was checked using the Doornik & Hansen (2008) omnibus. Principal Component Analysis (PCA) and Discriminant Function Analysis (DFA) were performed to specifically assess the degree of morphological differentiation among the members of *Isometrus* found in the Western Ghats. PCA was performed using 20 morphometric parameters taken from adult males. Factor scores of the first two Principal Components (PC) were observed on a scatter plot. Furthermore, sets of 20 predictor variables were generated from the PCA and all the factor scores were used as input variables for performing a DFA, in order to also determine the classification success of the studied samples. PCA and DFA were performed using the statistical software PAST ver. 4.03 (Hammer *et al.* 2001).

The following characters were used for statistical analysis (L = length; W = width; D = depth): Carapace (W), Mesosoma (L), Mesosoma Tergite VII (L/W), Metasoma (L), Metasoma Segment I (W), Femur and Patella (L/W), Pedipalp Chela (L), Pedipalp Manus (W), Movable Finger (L), Telson Vesicle (L/W/D), Pectine and Genital Operculum (L/W).

Results

Molecular Phylogenetics (Figs 1–2)

All known species of the genus *Isometrus* found in India were included in our phylogenetic analysis of a 525 bp fragment of the *COI* and a 500 bp fragment of the *16S* mitochondrial genes. ML and BI analyses generated trees with different topologies, but both new species and *I. sankeriensis* were each recovered as monophyletic with high ultrafast bootstrap support in the ML analysis (>99) and high posterior probability values in the BI analysis (*pp* = 1). A cluster containing two sequences from specimens from the type locality of *I. sankeriensis* were recovered as sister to *I. amboli* and an undescribed species from Dandeli, Karnataka, in both analyses. All specimens of the species from Wayanad (Kerala) were recovered as monophyletic in both analyses and were recovered as sister to a clade comprising *I. thurstoni* and *I. kovariki* in the ML and BI analyses. All specimens of the species from Kadmane Tea Estate, Karnataka, which is described here, were recovered as monophyletic in both analyses; however, this species was recovered as sister to a clade containing all the remaining Indian species of *Isometrus*, excluding *I. maculatus* in the ML analysis, while it is sister to *I. maculatus* in the BI analysis.

Genetic divergence (*p*-distance) (Tables 6–7)

All species of *Isometrus* showed moderate to high genetic divergence based on the 525 bp fragment of the *COI* mitochondrial gene. *I. sankeriensis* separated from *I. amboli* with a minimum genetic divergence of 4.7%, but showed 5.1–14.2% divergence from all other congeners. The species from Wayanad (Kerala) separated from *I. sankeriensis* with a minimum genetic divergence of 9.1%, but showed 9.1–14.0% divergence from other congeners. The species from Kadmane Tea Estate, Karnataka separated from

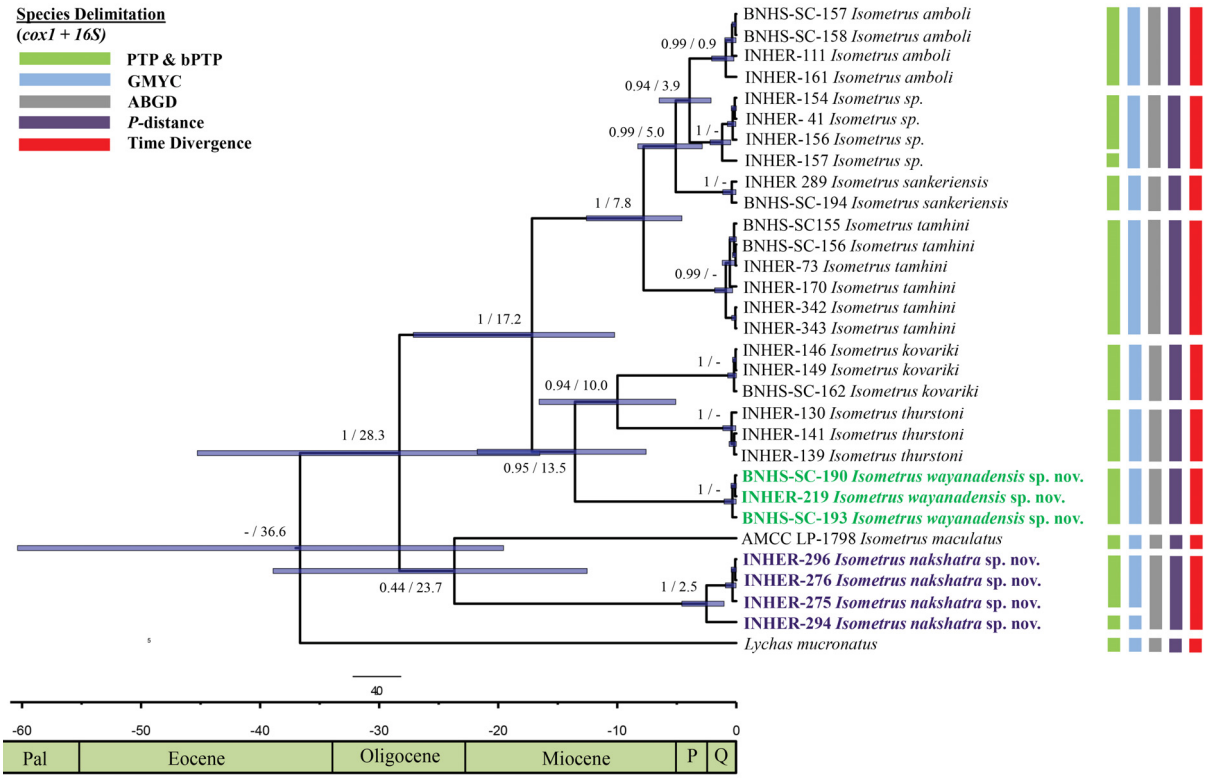

Fig. 1. Ultrametric tree showing phylogenetic relationships. Values along the nodes indicate Bayesian posterior probabilities and divergence dates in MY (PP/DD). Bars at the nodes indicate 95% HPD. Vertical bars represent delimitation analysis results.

I. sankeriensis with a minimum genetic divergence of 12.6% and showed 11.9–14.8% divergence from other Indian congeners.

All species of *Isometrus* showed moderate to high genetic divergence based on the 500 bp fragment of the *16S* mitochondrial gene. *I. sankeriensis* separated from *I. amboli* with a minimum genetic divergence of 2.6%, but showed 4.2–13.8% divergence from all other congeners. The species from Wayanad (Kerala) was closest to *I. thurstoni* and separated with a minimum genetic divergence of 7.0%, but showed 8.1–13.2% divergence from all other congeners. The species from Kadmane Tea Estate, Karnataka was closest to *I. thurstoni* and separated with a minimum genetic divergence of 12.5% and showed 12.7–14.5% divergence from other Indian congeners.

Species delimitation (Fig. 1)

PTP, bPTP and GMYC species delimitation analyses each identified ten distinct species groups within *Isometrus* with high support values. ABGD species delimitation analysis identified eight species clusters within *Isometrus*.

Based on the threshold of 3 Mya, nine species of *Isometrus* were delimited.

All these analyses support the presence of multiple new species from the Western Ghats of India and also support the revalidation of *I. sankeriensis*.

Geographical separation (Fig. 26A)

There is a clear geographical separation among all species of *Isometrus* found in India. Based on the topologies of the ML and BI analyses, species from northern WG form an independent lineage distinct

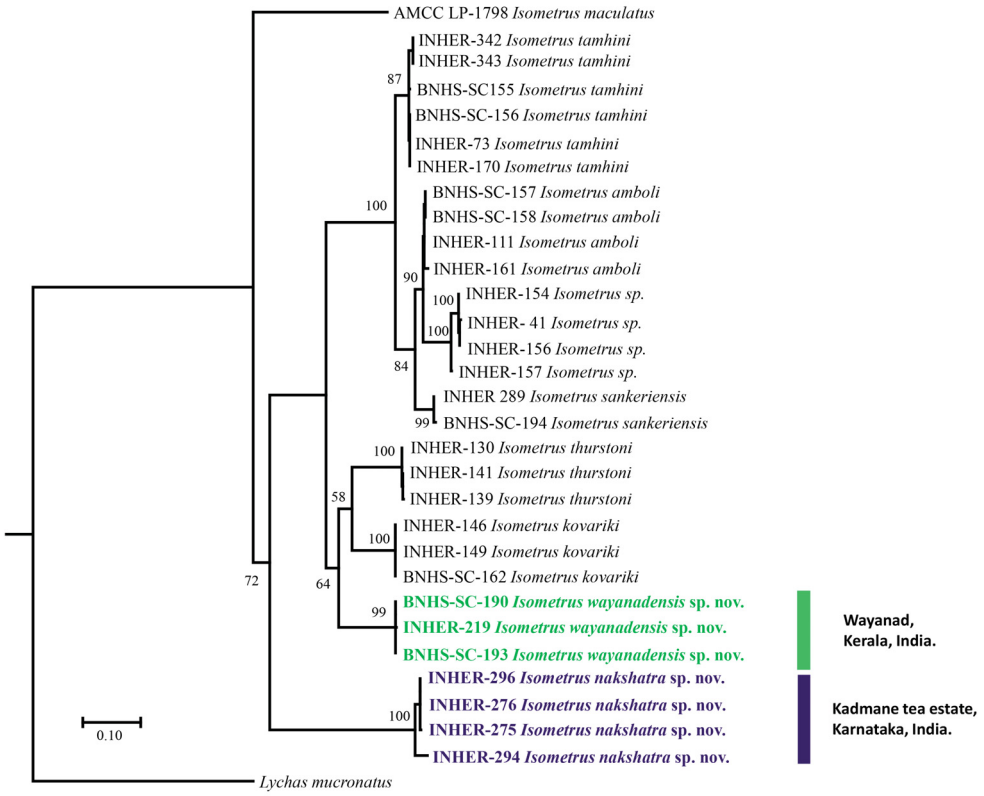

Fig. 2. Maximum Likehood phylogenetic tree (ML) for *Isometrus* Ehrenberg, 1828. Values along the nodes are bootstraps for 1000 iterations.

Table 6. Pairwise uncorrected raw distances (%) expressed as minimum–maximum based on COI gene sequences for Indian species of *Isometrus* Ehrenberg, 1828. Values in brackets are intra-clade distances.

Species	IM	IT	IA	IK	IS	ISP	ITH	IW	IN	LM
Isometrus maculatus (IM)	[0.0]									
Isometrus tamhini (IT)	14.2–14.4	[0.0–0.6]								
Isometrus amboli (IA)	13.8–14.2	6.6–7.2	[0.0–0.8]							
Isometrus kovariki (IK)	16.5	9.7–9.9	10.1	[0.0]						
Isometrus sankeriensis (IS)	14.0–14.2	7.2–7.4	4.7–5.4	10.1	[0.0–0.4]					
Isometrus sp. (ISP)	13.0–14.0	6.8–7.4	3.8–5.4	10.6–12.2	5.1–6.2	[0.2–1.7]				
Isometrus thurstoni (ITH)	13.8–14.2	11.1–12.0	12.6–13.2	10.1–10.5	13.6–14.2	12.3–13.4	[0.2–0.4]			
Isometrus wayanadensis sp. nov. (IW)	13.8–14.0	10.9–11.3	11.1–11.8	11.8–12.0	10.5–10.9	9.1–10.3	12.0–12.4	[0.0–0.2]		
Isometrus nakshatra sp. nov. (IN)	13.2–14.4	12.8–13.2	12.8–13.6	14.6–14.8	12.6–12.8	11.9–13.6	14.2–14.8	13.2–14.2	[0.0–3.3]	
Lychas mucronatus (LM)	14.4	16.7–17.1	16.3–17.1	18.4	16.9–17.1	16.0–16.5	17.5–17.9	14.6–14.8	15.7–16.5	[0.0]

Table 7. Pairwise uncorrected raw distances (%) expressed as minimum–maximum based on 16S gene sequences for Indian species of *Isometrus* Ehrenberg, 1828. Values in brackets are intra-clade distances.

Species	IM	IT	IA	IK	IS	ISP	ITH	IW	IN	LM
Isometrus maculatus (IM)	[0.0]									
Isometrus tamhini (IT)	13.4	[0.0]								
Isometrus amboli (IA)	13.8	3.7	[0.0]							
Isometrus kovariki (IK)	13.2	10.3	10.5	[0.0]						
Isometrus sankeriensis (IS)	13.8	4.2	2.6	9.6	[0.0]					
Isometrus sp. (ISP)	14.3	4.2–5.5	3.1	10.5	4.2	[0.0]				
Isometrus thurstoni (ITH)	12.3	9.0	9.0	7.5	10.1	10.5	[0.0]			
Isometrus wayanadensis sp. nov. (IW)	13.2	10.1	9.6	8.1	10.5	10.1	7.0	[0.0]		
Isometrus nakshatra sp. nov. (IN)	12.7–12.9	14.0	13.8	13.8	13.6	14.0–14.5	12.5	13.2	[1.5]	
Lychas mucronatus (LM)	21.7	21.9	21.7	20.0	20.8	21.3–21.5	20.8	21.7	19.3	[0.0]

from species found in the southern WG. Based on this study, all species in India seem to have small ranges and be allopatric in distribution, except for *I. maculatus*, but the wide ranging distribution of this species needs to be confirmed with more sampling and genetic data. Populations of *Isometrus* are known to exist from low elevation coastal scrub forest to high elevation evergreen forest in the WG, with a wide range of temperatures and precipitation (Fig. 26).

Morphological separation based on statistical analysis (Fig. 3)

Size-corrected morphometric data was not significantly different from the multivariate normal (Doornik and Hansen omnibus, within group Ep = 131.4, P < 0.0001). Three species, *I. tamhini*, *I. sankeriensis* and *I. nakshatra* sp. nov., formed relatively distinct clusters, whereas *I. wayanadensis* sp. nov., *I. kovariki*, *I. amboli* and *I. thurstoni* failed to separate out on the first two PCA factor planes that had eigenvalues > 1.0 and explained 91.06% of variation among the species (Fig. 3). Two morphometric parameters, mesosoma tergite length (MTL) and metasoma segment length (MSL) account for most of the variance measured in PCA factor 1, while three morphometric parameters, pedipalp femur length (PFL), pedipalp patella length (PPL) and chela length (CL), represent most of the variance for PCA factor 2. Furthermore, our DFA resulted in 100% classification success, with all the individual samples being classified into their respective species (Table 8), except for *I. kovariki* and *I. wayanadensis*, and *I thurstoni* and *I. amboli*, which have overlapping distributions on the morphological landscape. First, four discriminant function roots showed eigenvalues > 1.0 and explained 97.89% of the variations among these species. Overall, the PCA and DFA results showed morphological differentiation among most of the analysed species and were considered reliable for the recognition of new species based on the morphometric data.

Total number of species

On the basis of phylogeny, genetic divergence, species delimitation methods, geographical separation and morphological separation based on statistical analysis, three novel monophyletic groups were discovered from the Western Ghats of India. However, due to low sample size for one of the novel lineages delineated in this study (*Isometrus* sp. INHER 154, INHER 41, INHER 156 and INHER 157

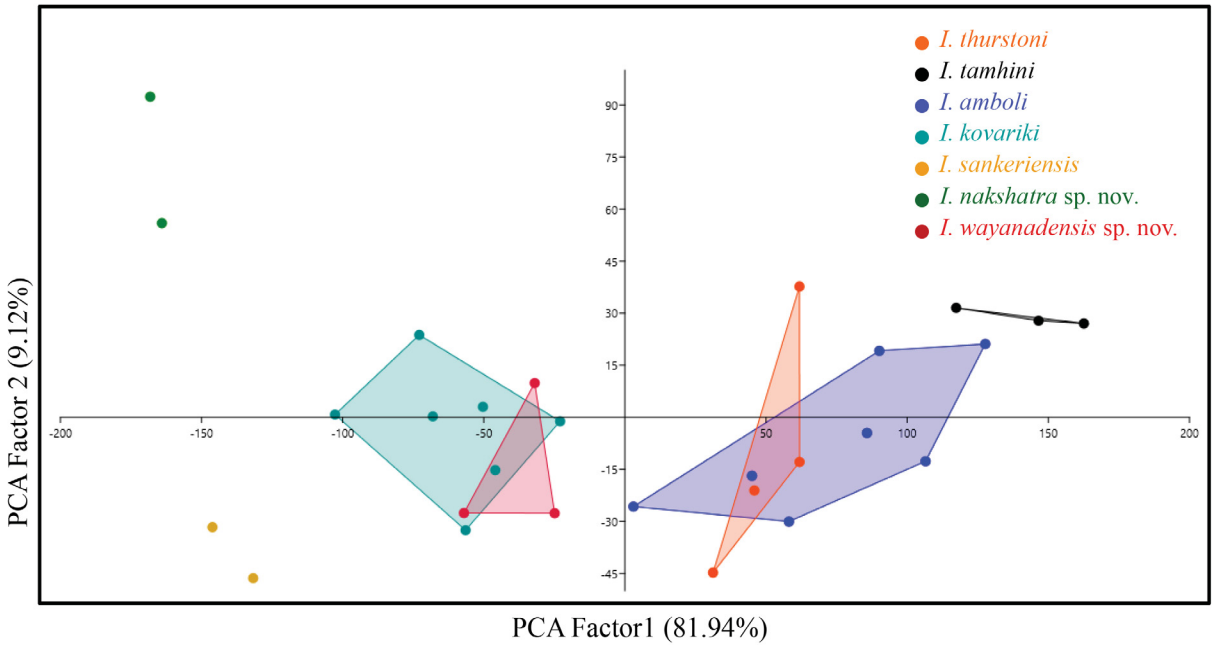

Fig. 3. Projection of first two Principle Component factors explaining 91.06% of the variation among the seven species of the genus *Isometrus* Ehrenberg, 1828.

Table 8. Classification matrices for discriminant function analysis.

Species	IT	IA	ITH	IK	IN	IW	IS	Total
I. tamhini (IT)	3	0	0	0	0	0	0	3
I. amboli (IA)	0	7	0	0	0	0	0	7
I. thurstoni (ITH)	0	0	4	0	0	0	0	4
I. kovariki (IK)	0	0	0	7	0	0	0	7
I. naksatra sp.nov (IN)	0	0	0	0	2	0	0	2
I. wayanadensis sp.nov (IW)	0	0	0	0	0	3	0	3
I. sankeriensis (IS)	0	0	0	0	0	0	2	2
Total	3	7	4	7	2	3	2	28

from Dandeli and Anshi in Karnataka), we choose to describe only two of these novel lineages, from Kadmane Tea Estate, Karnataka, and Wayanad, Kerala, as distinct species. Below, we provide full descriptions of the two new species and also provide a diagnosis and re-description of *I. sankeriensis*, which is here revalidated. This study thus elevates the total number of species of *Isometrus* found in India to eight.

Systematics

Phylum Arthropoda Von Siebold, 1848
Class Arachnida Lamarck, 1801
Order Scorpiones C.L. Koch, 1837
Family Buthidae C.L. Koch, 1837

Genus ***Isometrus*** Ehrenberg, 1828
Figs 1–26; Tables 1–8

Type species

Scorpio maculatus (DeGeer, 1778).

Diagnosis (♂♀)

Carapace without carinae. Lateral ocular tubercle with type 5 ocelli and median ocular tubercle with one pair of ocelli. Sternum type 1, triangular in shape. Ventral aspect of tarsomere II of leg IV with two dense rows of setae. Pedipalps orthobothriotaxic, type Aβ. Trichobothrium *db* of fixed finger of chela located between *dt* and *et*. Legs without tibial spurs on tibiae III and IV. Movable finger and fixed finger of chela with six rows of prolateral and retrolateral denticles in pairs and one additional single retrolateral denticle on proximal portion. Mesosoma I–VI tergites each with single median carina. All metasomal segments longer than wide. Telson vesicle always longer than wide, with subaculear nodule.

Sexual dimorphism

All species of *Isometrus* in India exhibit similar sexual dimorphism. Males have longer and more slender pedipalps as opposed to females. Males have a slightly more elongated telson vesicle than females. The aculeus of the telson in females is more curved and elongated than in males. The male genital operculum bears a pair of small genital papillae posteriorly. In females the genital operculum is divided by a median suture covering the female genital orifice.

Isometrus sankeriensis Tikader & Bastawade, 1983
Figs 4–7, 18A, 19A, E, 26A, D, 21A, 23A, 25A; Table 1

Isometrus (*Closotrichus*) *sankeriensis* Tikader & Bastawade, 1983: 311.

Isometrus (*Isometrus*) *sankeriensis* – Kovařík 1994: 201; 1997: 8; 2003: 4. — Fet & Lowe 2000: 150.

Diagnosis (♂)

Total length 31.33–35.14 mm. Base colouration yellowish-brown and variegated with black-brown stripes and spots. Basal segments of chelicerae dorsally yellowish with blackish reticulation. Pectinal tooth number 15–18. Median supra ocular region with some coarse and some fine granules. Median ocelli anteriorly situated, with ratio 1 : 2.2 (ratio of median ocelli to anterior margin/median ocelli to posterior margin). Tergites I–VI finely granular with strong median carina. All segments of metasoma longer than wide. *Isometrus sankeriensis* differs from all other Indian species of *Isometrus* based on the following set of morphological characters:

1. Surface of carapace coarsely and sparsely granular with some areas without granules (Figs 5C, 18A) as opposed to: coarsely and densely granular in *I. tamhini*; finely and densely granular in *I. amboli*; granular throughout with mixed granules, more closely granular in inter-ocular area and median posterior ocular area in *I. kovariki*; and granular throughout but obsolete in *I. maculatus*.
2. Chela length to width ratio in males 5.7–5.8 as opposed to 6.1–6.5 in *I. tamhini* and 5.0–5.2 in *I. thurstoni* (Tables 1–3).
3. Lateral patches on mesosomal tergites V and VI with fine granulation along margins (Fig. 21A) as opposed to coarse granulation along margins in *I. tamhini*.
4. Metasomal length to carapace length ratio in males 5.9–6.1 as opposed to 8.8–9.1 in *I. tamhini*, 7.2–8.8 in *I. amboli*, 7.6–8.2 in *I. thurstoni,* 6.5–7.3 in *I. kovariki* and 9.6 in *I. maculatus* (Tables 1–3).
5. Lateral supramedian and ventral lateral carinae on metasomal segments II–IV strongly granular (Fig. 23A), as opposed to moderately to weakly granular in *I. amboli*, *I. thurstoni* and *I. kovariki*.
6. Telson length to width ratio in males 4.3 opposed to 3.7–4.0 in *I. thurstoni* (Tables 1–3).
7. Ventral median carina on telson vesicle weakly granular (Fig. 19D) as opposed to strongly granular in *I. tamhini* and moderately granular in *I. amboli.*
8. Spiniform granules of promedian carina of pedipalp patella moderately developed as opposed to strongly developed in *I. thurstoni* (Figs 24–25).

For comparisons of *I. sankeriensis* with the proposed new species described below in this study, refer to the diagnosis section of those respective new species.

Material examined

Holotype

INDIA • ♂, adult; Karnataka State, Uttar Kannada, Karwar, Sunkeri [misspelled as Sankeri]; 25 Dec. 1975; U.A. Gajbe leg.; ZSI 5088/18.

Comments

The authors believe that the holotype of *I. sankeriensis* (adult male) (ZSI 5088/18) is lost as it was not traceable in any ZSI centres. To stabilize the taxonomy of the genus, we found it necessary to designate a neotype using the specimen under the voucher number BNHS SC 194. The neotype meets all the requirements of Article 75 of ICZN as it was collected from the exact type locality Sunkeri (erroneously given as Sankeri in Tikader & Bastawade 1983), Karwar, Karnataka, India. Our description of the neotype matches the description of the holotype in Tikader & Bastawade (1983). The allotype of *I. sankeriensis* (immature female) (ZSI 5089/18), collected in the Silent Valley Forest, Kerala, India,

which is presumably also lost as it was not traceable in any ZSI centres, could be a different species considering the limited distributional ranges of species of *Isometrus* in India; however, this needs to be confirmed.

Neotype (designated here)
INDIA • ♂, adult; Karnataka State, Uttar Kannada, Karwar, Sunkeri; 14.80° N, 74.18° E; 30 m a.s.l.; 30 Aug. 2019; Makarand Ketkar, Shauri Sulakhe, Shubhankar Deshpande and Mayuresh Kulkarni leg.; BNHS SC 194.

Other material
INDIA • 1 ♂, adult; same locality as for neotype; 4 Nov. 2020; Makarand Ketkar, Shauri Sulakhe, Shubhankar Deshpande and Swayam Thakkar leg.; INHER 288.

Description (neotype, ♂, measurements in Table 1)

Colouration (Fig. 4A–B). Body and appendages yellowish brown and variegated with blackish brown stripes and spots; metasomal segment V yellowish to dark brownish, darker on posterior portion; pedipalp fingers dark brownish at base. Ventral surfaces uniformly yellow and sternite VII with very few dark spots. Basal segments of chelicerae yellowish dorsally with blackish reticulation ending anteriorly in a blackish transverse patch; ventral portion of chelicerae yellowish brown; fingers of chelicerae yellowish brown with tip of fingers blackish brown. Telson yellowish to dark brownish.

Carapace (Figs 5C, 18A). Surface coarsely and sparsely granular with some areas without granules. Carapace without carinae, median supra-ocular area with some coarse and some fine granules. Pair of median ocelli situated anteriorly, with median ocelli to anterior margin/median ocelli to posterior margin ratio of 1 : 2.2. Antero-lateral ocular tubercle granular with type 5 lateral ocelli. Three pairs of large major ocelli and two small minor ocelli situated behind major ocelli. Median longitudinal furrow throughout carapace. Lateral margins finely crenulated below lateral ocelli. Posterior margin almost entirely smooth.

Chelicerae (Fig. 4D). Characteristic of Buthidae. Basal segments and movable fingers with short and firm setae on basal and ventral surfaces.

Pedipalps (Figs 6, 25A). Femur with five carinae (prodorsal, retrodorsal, promedian, retromedian and proventral). All carinae crenulated. Intercarinal surfaces smooth except ventral surface with a few dense granules on proximal portions. Patella with seven distinct carinae (dorsomedian, prodorsal, retrodorsal, retromedian, retroventral, promedian and proventral). Intercarinal surfaces almost entirely smooth on ventral surface and weakly granular on dorsal surface. Chela acarinate. Fixed finger with one smooth and obsolete dorsal median and retrodorsal carina. Movable and fixed fingers with six rows of prolateral and retrolateral denticles in pairs and one additional single row of retrolateral denticles on proximal portion. Trichobothrial pattern typical for genus (chela dorsal 12, chela ventral 2, patella dorsal 6, patella retrolateral 7, femur dorsal 7 and femur prolateral 4).

Legs (Fig. 4A–B). Femur and patella carinated. All carinae granular. Tibiae III and IV carinated, without tibial spurs. All legs with a pair of pedal spurs. Tarsomere covered with long delicate setae arranged in parallel rows on ventral side. Tarsomere I (basitarsus) carinated dorsally with tuft of short, stout blackish setae on ventral side. Tarsomere II (telotarsus) compressed laterally and ventrally with paired row of short, pointed, anteriorly directed, closely placed setae.

Genital operculum (Fig. 4C). Wider than long, elliptical, separated, with a pair of short male genital papillae.

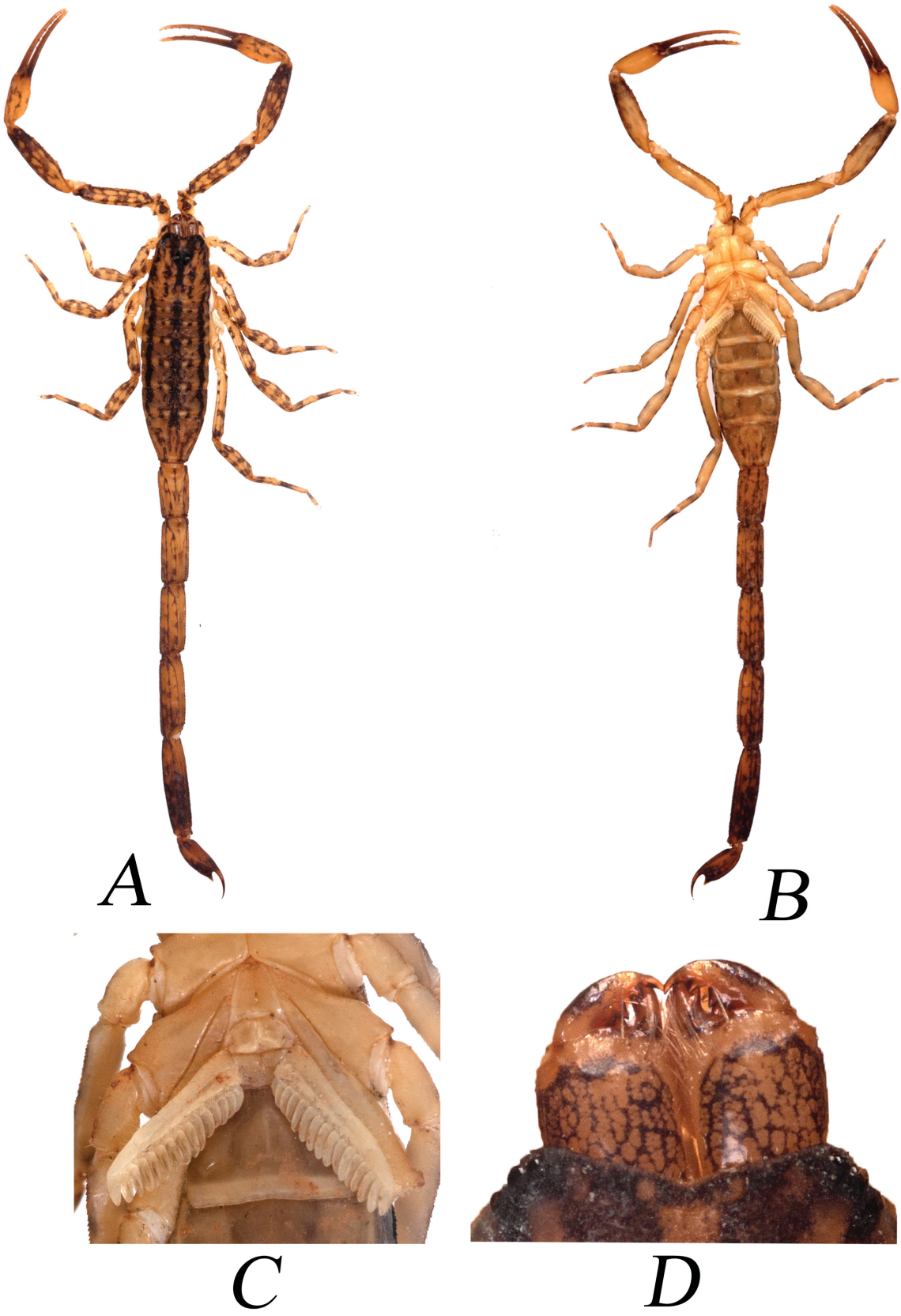

Fig. 4. *Isometrus sankeriensis* Tikader & Bastawade, 1983, neotype, adult ♂ (BNHS SC 194). **A**. Dorsal view. **B**. Ventral view. **C**. Sternopectinal area, dorsal view. **D**. Chelicerae, dorsal view.

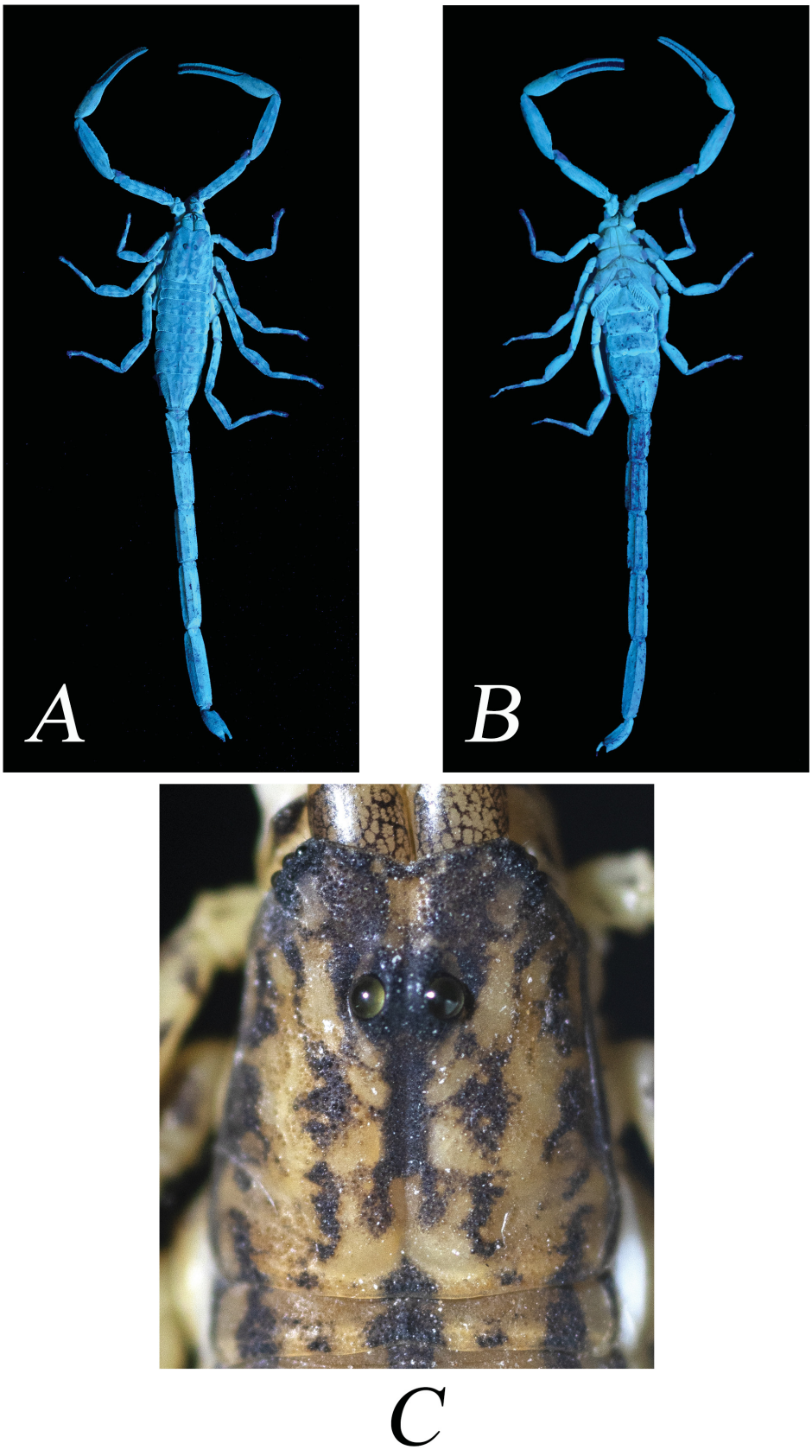

Fig. 5. *Isometrus sankeriensis* Tikader & Bastawade, 1983, neotype, adult ♂ (BNHS SC 194). **A**. Dorsal view, UV light. **B**. Ventral view, UV light. **C**. Carapace, white light.

Pectines (Fig. 4C). Basal piece rectangular, deeply notched on anterior median margin. Posterior margin of basal piece curved and smooth. Marginal lamellae of 3/3 digits and median lamellae of 6/7 digits, outer margin armed with a row of stout, short red setae and few setae on surface. Fulcra 14/15, roughly triangular, each armed with a few short red setae, placed in between adjacent pectinal teeth. Teeth 15/16, strong and stout.

Mesosoma (Figs 4A–B, 5A–B, 21A). Tergites I–VI finely granular with short median carina. Lateral patches on mesosomal tergites V and VI with fine granulation along posterior margins. Posterior and lateral margins granular. Tergite VII narrowed posteriorly, granular with two pairs of lateral granular carinae, diverging laterally. Broad median carina limited to posterior half. Sternites III–VI almost entirely smooth with a pair of spiracles. Sternite V exceptionally smooth and emarginated on median part. Sternite VII smooth on posterior margin, while finely crenulated to serrated on lateral margins; two pairs of granular carinae with median and lateral carinae present on posterior two-thirds.

Metasoma (Figs 4A–B, 5A–B, 23A). All segments longer than wide. Segment I with five pairs of granular carinae (dorsal lateral, lateral supramedian, lateral inframedian, ventral lateral and ventral submedian). Intercarinal surfaces weakly granular, anterior margin smooth. Segments II–IV with five pairs of carinae (dorsal lateral, lateral supramedian, ventral lateral, ventral submedian and lateral inframedian). Lateral supramedian and ventral lateral carinae strongly granular. Lateral inframedian carina granular, present only on posterior one-third. Intercarinal surfaces weakly granular, lateral supramedian and dorsal lateral carinae posteriorly ending in very weak subtriangular tubercles. Segment V with seven carinae (dorsal lateral, lateral supramedian and ventral lateral pairs and a single ventral median). Intercarinal surfaces more granular than on segments I–IV. Anal rim very weakly granular.

Fig. 6. *Isometrus sankeriensis* Tikader & Bastawade, 1983, neotype, adult ♂ (BNHS SC 194). **A–B**. Pedipalp chela. **A**. Dorsal view. **B**. Ventral view. **C–D**. Patella. **C**. Dorsal view. **D**. External view. **E–F**. Femur. **E**. Dorsal view. **F**. Internal view. Trichobothrial pattern indicated by yellow dots.

Fig. 7. Type locality of *Isometrus sankeriensis* Tikader & Bastawade, 1983. **A**. View of Sunkeri Road. **B**. View of semi-evergreen disturbed forest at the type locality.

Telson (Fig. 19A, D). With stout vesicle, bulbous on distal portion and smooth on dorsal surface. Lateral surface demarcated with weakly granular ridge. Ventral median carina weakly granular, ending in triangular, subaculear, pointed nodule, armed with two pairs of minute denticles on inner margin. Ventral portion with two pairs of sparsely and finely granular carinae. Intercarinal surfaces weakly granular. Aculeus elongated, sharp and moderately curved.

Distribution, habitat and ecology (Figs 7, 26)

Isometrus sankeriensis is currently known only from the type locality near Karwar, India. It is found in the degraded forests and scrub around Sunkeri village, Karwar. We also observed some individuals on the way to Jamba Falls near Sunkeri village. This forest habitat is under tremendous stress due to mass tourism and all factors commonly responsible for land degradation (Buckingham & Weber 2016). Our surveys recorded a small population of this species. The population also reaches the forest close to the buffer zone of Anshi National Park, which gives some hope for survival of this species. Currently the species appears to be distributed only in the lowlands in the coastal scrub forest around Karwar, Karnataka. However, more sampling from the protected area needs to be done to confirm the population density of this species. The ecology of this species is congruent with that of bark scorpions.

Remarks

Our diagnosis of *I. sankeriensis*, based on specimens we collected at the type locality, shows strong morphological divergence from that of *I. thurstoni*. The two species differ from each other based on the following morphometric ratios (Table 1, meristic and morphometric data sourced from Sulakhe *et al.* 2020a): chela length to width ratio in males of *I. sankeriensis* 5.7–5.8 as opposed to 5.0–5.2 in *I. thurstoni*; metasomal length to carapace length ratio in males of *I. sankeriensis* 5.9–6.1 as opposed to 7.6–8.2 in *I. thurstoni*; telson length to width ratio in males of *I. sankeriensis* is 4.3 opposed to 3.7–4.0 in *I. thurstoni*. The two species also differ in qualitative characters: lateral supramedian and ventral lateral carinae on metasomal segments II–IV strongly granular in *I. sankeriensis* as opposed to weakly granular in *I. thurstoni* (Figs 22A, 23A); spiniform granules of promedian carina of pedipalp patella moderately developed as opposed to strongly developed in *I. thurstoni*. The two species differ from each other by a raw genetic divergence of 13.6–14.2% based on *COI* and 10.1% on *16S* (Tables 6–7). In consideration of all the above evidence, we resurrect *I. sankeriensis*.

Isometrus nakshatra sp. nov.
urn:lsid:zoobank.org:act:E3BBB5E4-8A30-40DD-9BBD-731046A22232
Figs 8–12, 18B, 19B, E, 21B, 23B, 25B; Table 2

Diagnosis (♂♀)

Total length 38.60–48.69 mm. Base colouration blackish-brown and variegated with brown-yellow stripes and spots; appendages yellowish with blackish-brown stripes and spots. Basal segments of chelicerae dorsally dark brown with blackish reticulation. Pectinal tooth number 15–16 in both sexes. Median supra-ocular region with fine and dense granulation. Median ocelli anteriorly situated in ratio of 1 : 1.9. Tergites I–VI sparsely and coarsely granular, with median carina stronger on posterior region. *Isometrus nakshatra* sp. nov. differs from all other Indian species of *Isometrus* based on the following set of morphological characters:

1. Surface of carapace with mixed granulation with fine and dense granulation in median supra-ocular region (Figs 9C, 18B) as opposed to: coarsely and sparsely granular with some areas without granules in *I. sankeriensis* and *I. thurstoni*; finely and densely granular in *I. amboli*; coarsely and densely granular in *I. tamhini*; granular throughout with mixed granules, more densely granular in inter-

ocular area and median posterior ocular area in *I. kovariki*; and granular throughout but obsolete in *I. maculatus*.
2. Chela length to width ratio in males 10.6 as opposed to 6.1–6.5 in *I. tamhini*, 5.3–5.9 in *I. amboli*, 5.7–5.8 in *I. sankeriensis*, 5.1–6.4 in *I. kovariki* and 5.0–5.2 in *I. thurstoni*; in females 6.1–6.2 as opposed to 5.2–5.9 in *I. tamhini*, 5.7 in *I. amboli* and 4.8 in *I. kovariki* (Tables 1–3).
3. Lateral patches on mesosomal tergites V and VI with fine granulation along margins (Fig. 21B) as opposed to coarse granulation along margins in *I. tamhini.*
4. Metasomal length to carapace length ratio in males 5.3–5.8 as opposed to 8.8–9.1 in *I. tamhini*, 7.2–8.8 in *I. amboli*, 5.9–6.1 in *I. sankeriensis*, 7.6–8.2 in *I. thurstoni*, 6.5–7.3 in *I. kovariki* and 9.6 in *I. maculatus* (Tables 1–3).
5. Lateral supramedian and ventral lateral carinae on metasomal segments II–IV moderately granular (Fig. 23B) as opposed to strongly granular in *I. tamhini* and *I. sankeriensis.*
6. Telson length to width ratio in males 3.5–4.1 as opposed to 4.6–4.8 in *I. tamhini* and 4.3 in *I. sankeriensis* (Tables 1–3).
7. Ventral median carina of telson vesicle weakly granular (Fig. 19E) as opposed to moderately granular in *I. amboli* and strongly granular in *I. tamhini*.
8. Spiniform granules of promedian carina of pedipalp patella weakly developed as opposed to moderately developed in *I. tamhini*, *I. amboli*, *I. sankeriensis* and *I. kovariki*, and strongly developed in *I. thurstoni* (Figs 24–25).

For comparisons of *I. nakshatra* sp. nov. with *I. wayanadensis* sp. nov., described below, refer to the diagnosis section of the latter.

Etymology

The species epithet is a noun in apposition, derived from the Kannad word 'nakshatra' (= 'star'). It refers to the star-shaped fort named 'Manjarabad', very close to the type locality. The fort was built in 1792 by Tipu Sultan, the then ruler of Mysore, using French military architects. The sultan wanted to build a highway between Mangalore and Coorg for his expansion programs. As he was allied with the French at that time against the British, he sought the help of French engineers to build this fort in European style.

Material examined

Holotype

INDIA • ♂, adult; Karnataka State, Hassan District, Sakleshpur, Kadmane Tea Estate; 12.89° N, 75.68° E; 911 m a.s.l.; 2 Nov. 2020; Makarand Ketkar, Shubhankar Deshpande, Shauri Sulakhe and Swayam Thakkar leg.; BNHS SC 195.

Paratypes

INDIA • 1 ♂, adult; same collection data as for holotype; INHER 275 • 1 ♀, adult; same collection data as for holotype; INHER 276 • 1 ♀, adult; same collection data as for holotype; BNHS SC 196.

Description (holotype, ♂, measurements in Table 2)

Colouration (Fig. 8A–B). Body blackish brown and variegated with brownish yellow stripes and spots; appendages yellowish with blackish brown stripes and spots; metasomal segment V dark brownish to blackish, darker on posterior portion; pedipalp fingers dark brownish. Ventral portion uniformly brown and sternite VII with a few dark spots. Basal segments of chelicerae dorsally dark brown with blackish reticulation, ending anteriorly in a blackish transverse patch. Fingers of chelicerae dark brown with tip of fingers black. Telson yellowish-brown.

Carapace (Figs 9C, 18C). Surface of carapace with mixed granulation. Carapace without carinae. Median supra-ocular area finely granular. Inter-ocular area with coarse and dense granules. Pair of median ocelli

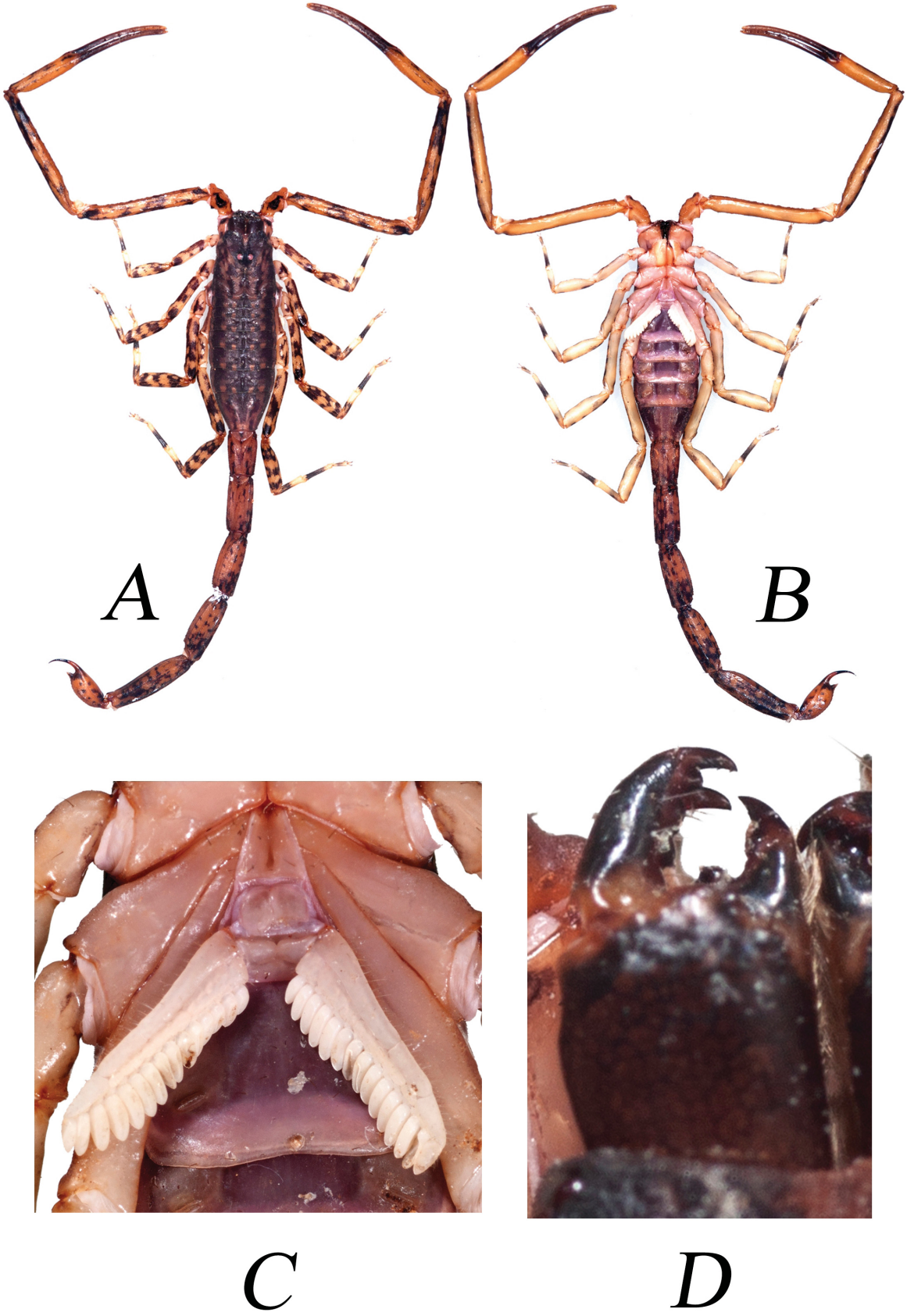

Fig. 8. *Isometrus nakshatra* sp. nov., holotype, adult ♂ (BNHS SC 195). **A**. Dorsal view. **B**. Ventral view. **C**. Sternopectinal area. **D**. Chelicera, dorsal view.

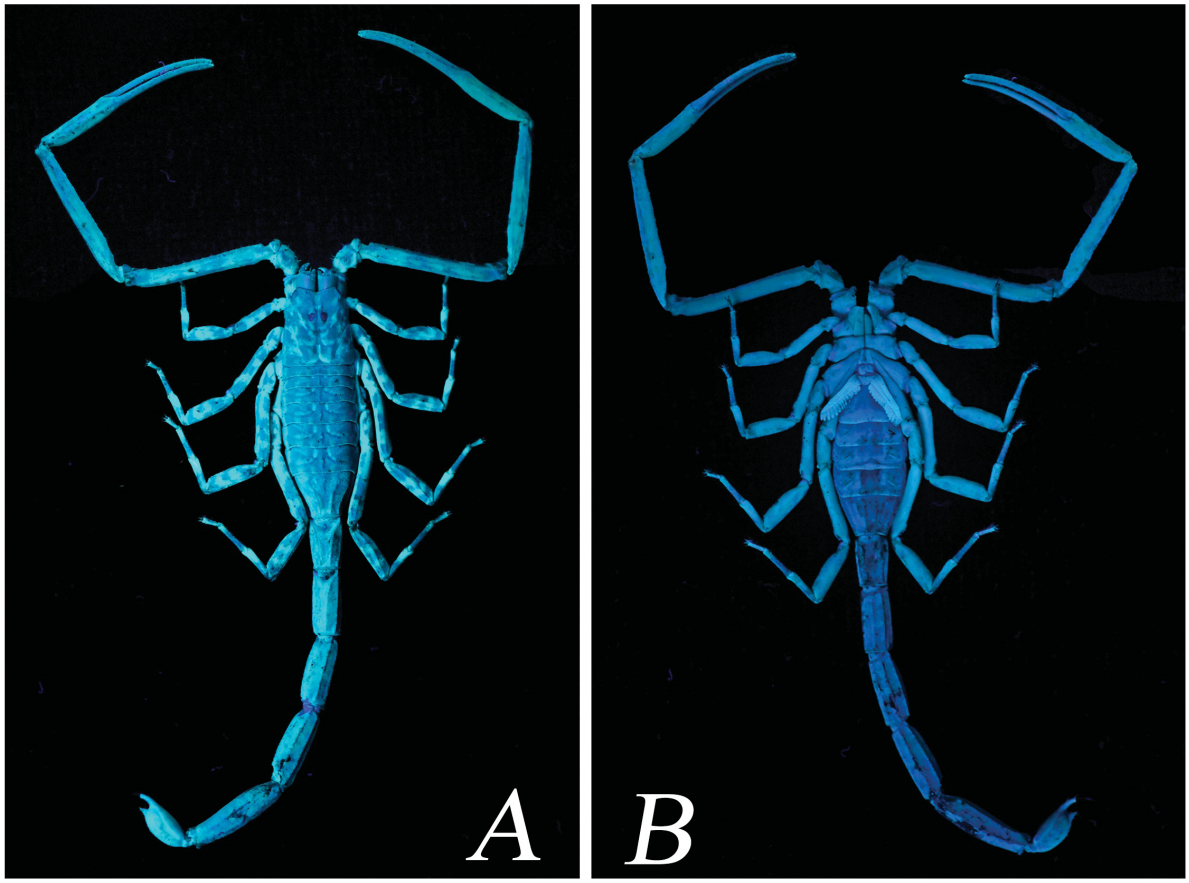

C

Fig. 9. *Isometrus nakshatra* sp. nov., holotype, adult ♂ (BNHS SC 195). **A**. Dorsal view, UV light. **B**. Ventral view, UV light. **C**. Carapace, white light.

situated anteriorly, with median ocelli to anterior margin/median ocelli to posterior margin ratio of 1 : 1.9. Antero-lateral ocular tubercle granular with type 5 lateral ocelli. Three pairs of large major ocelli and two small minor ocelli situated behind major ocelli. Longitudinal furrow shallow. Anterior margins finely granular. Lateral margins weakly crenulated below lateral ocelli. Posterior margin almost entirely smooth.

Chelicerae (Fig. 8C). Characteristic of Buthidae. Basal segments and movable fingers with short and firm setae on basal and ventral surfaces.

Pedipalp (Figs 10, 25B). Femur with five carinae (prodorsal, retrodorsal, promedian, retromedian and proventral). All carinae crenulated. Intercarinal surfaces weakly granular except ventral surface smooth with a few fine granules on proximal portions. Patella with seven distinct carinae (dorsomedian, prodorsal, retrodorsal, retromedian, retroventral, promedian and proventral). Intercarinal surfaces weakly granular on dorsal surface and smooth on ventral surface. Chela with four carinae (dorsomedian, dorsoretrosubmedian accessory, retromedian and retroventral). Fixed fingers with two smooth dorsal median and retrodorsal carinae. Movable and fixed fingers with six rows of prolateral and retrolateral denticles in pairs and one additional single row of retrolateral denticles on proximal portion. Trichobothrial

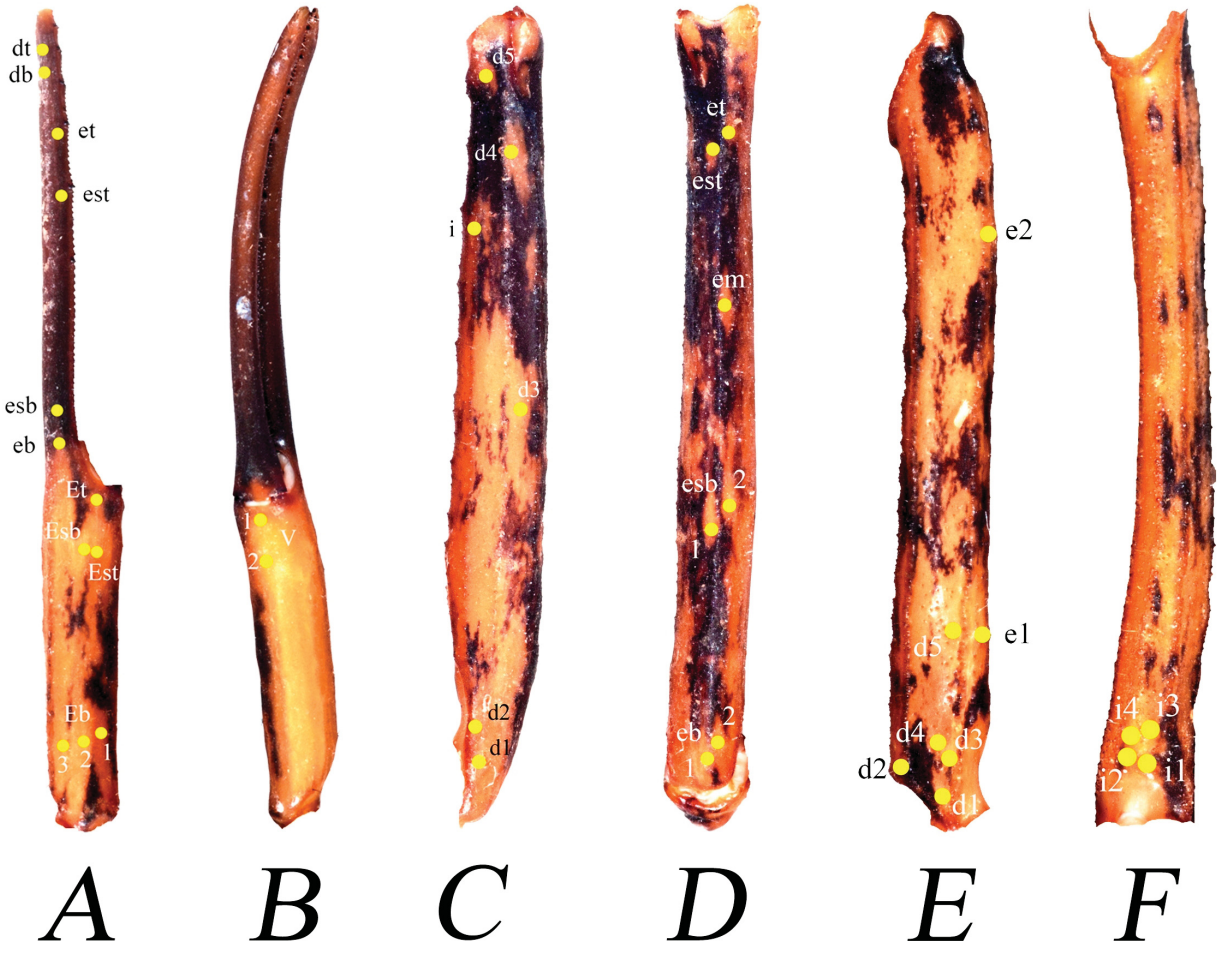

Fig. 10. *Isometrus nakshatra* sp. nov., holotype, adult ♂ (BNHS SC 195). **A–B**. Pedipalp chela. **A**. Dorsal view. **B**. Ventral view. **C–D**. Patella. **C**. Dorsal view. **D**. External view. **E–F**. Femur. **E**. Dorsal view. **F**. Internal view. Trichobothrial pattern indicated by yellow dots.

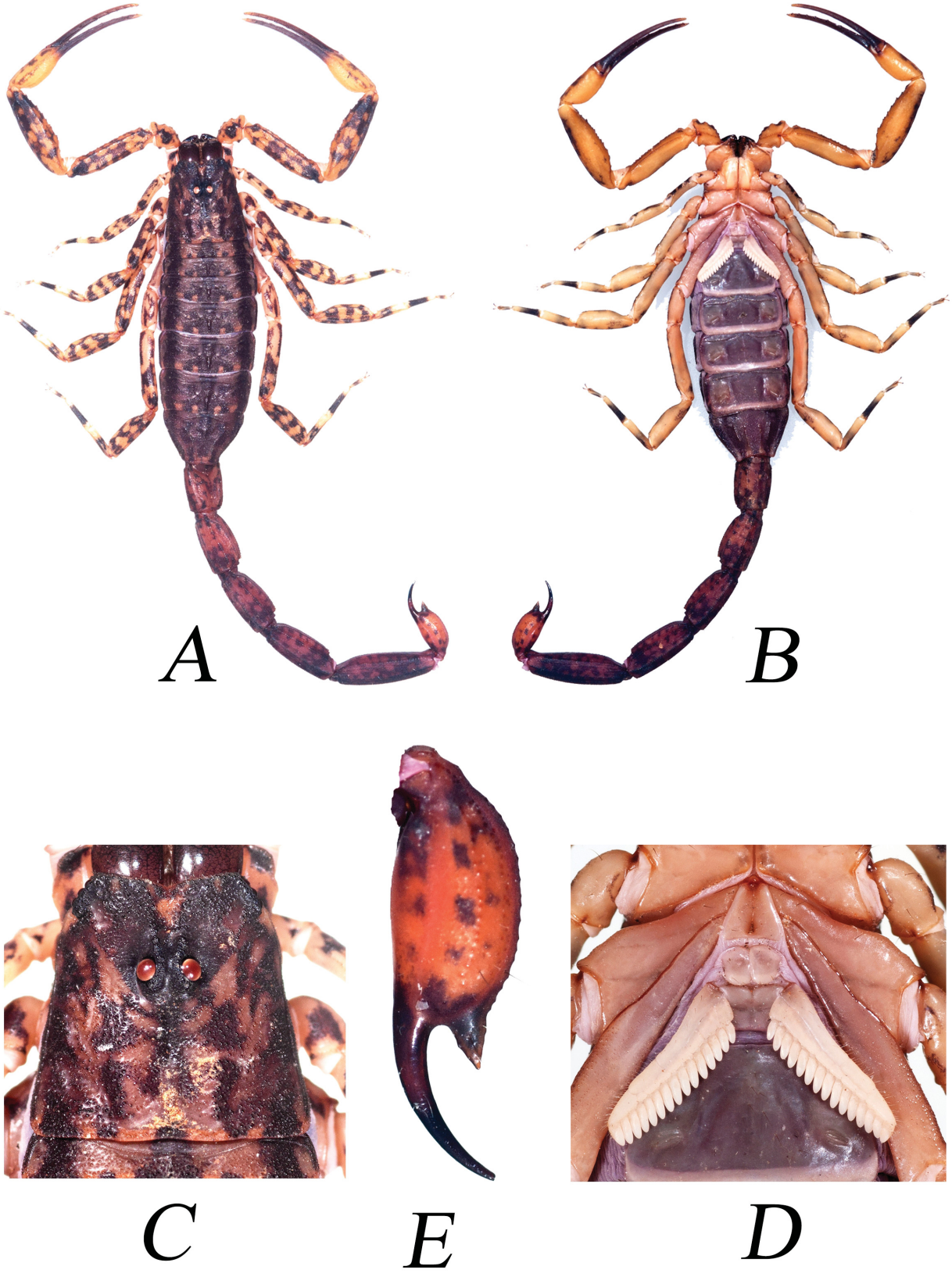

Fig. 11. *Isometrus nakshatra* sp. nov., paratype, adult ♀ (BNHS SC 196). **A**. Dorsal view. **B**. Ventral view. **C**. Carapace, dorsal view. **D**. Sternopectinal area. **E**. Telson, lateral view.

pattern typical for genus (chela dorsal 12, chela ventral 2, patella dorsal 6, patella retrolateral 7, femur dorsal 7 and femur prolateral 4).

Legs (Figs 8A–B, 9A–B). Femur and patellae carinated. All carinae granular. Tibia 3 and 4 without tibial spurs. All legs with pair of pedal spurs. Tarsomere covered with long delicate setae arranged in parallel rows on ventral side. Tarsomere I (basitarsus) with a tuft of short, stout blackish setae on ventral side. Tarsomere II (telotarsus) compressed laterally and ventrally, with paired row of short, pointed, anteriorly directed, closely placed setae.

Genital operculum (Fig. 8C). Wider than long, elliptical, separated with a pair of short male genital papillae.

Pectines (Fig. 8C). Basal piece rectangular, notched on anterior median margin. Posterior margin of basal piece curved. Marginal lamella of 3/3 digits and median lamella of 7/7 digits, outer margin armed with a row of stout, short red setae and a few setae on surface. Fulcra 14/14, very small, roughly triangular, each armed with a few short red setae, placed in between adjacent pectinal teeth. Teeth 15/15, strong and stout.

Mesosoma (Figs 8A–B, 9A–B, 21B). Tergites I–VI sparsely and coarsely granular with median carina more strongly developed on posterior side. Posterior and lateral margins granular. Lateral patches on mesosomal tergites V and VI with fine granulation along margins. Tergite VII granular, narrowed posteriorly, with two pairs of lateral granular carinae. Broad median carina present, more strongly developed on anterior portion. Sternites III–V almost entirely smooth, with a pair of spiracles. Sternite VI finely granular on lateral portion. Sternite VII entirely granular, more closely granular on lateral portion; two pairs of granular carinae, with median carina present on posterior portion and lateral carina present only on anterior half.

Metasoma (Figs 8A–B, 9A–B, 23B). All segments longer than wide. Segments I–IV with four pairs of carinae (dorsal lateral, lateral supramedian, ventral lateral, ventral submedian). Intercarinal surfaces almost smooth. Lateral supramedian and ventral lateral carinae on segments II–IV moderately granular. Lateral inframedian carina weakly developed on distal portion of segments III and IV. Dorsal lateral carina on segments I–IV ending in very weak tubercles. Segment V with five carinae (lateral supramedian pair, ventral lateral pair and single ventral median). Intercarinal surfaces granular. Anal rim granular.

Telson (Fig. 19B, E). With stout vesicle, smooth on dorsal surface. Ventral median carina weakly granular, ending in triangular, subaculear, pointed nodule, armed with a pair of minute denticles on inner basal margin. Ventral portion with two weak carinae. Lateral and ventral intercarinal surfaces weakly granular. Aculeus strongly elongated.

Distribution, habitat and ecology (Figs 12, 26)

Isometrus nakshatra sp. nov. is only known from its type locality, Kadmane Tea Estate, Sakleshpur, Hassan District, Karnataka State, India. Specimens were collected from undergrowth and tree bark in a small patch of disturbed evergreen forest on a hill slope adjacent to the crest line of the WG. Unlike other species of *Isometrus* from India, this new species was also observed in shrubby undergrowth along with tree bark. The forest patch here is disturbed and fragmented due to the infrastructure of the Kadmane tea factory and large scale agriculture (tea, coffee and pepper plantations). The ecology of the new species is congruent with that of bark scorpions.

Fig. 12. Type locality of *Isometrus nakshatra* sp. nov. **A**. View of dense evergreen forest along road at the type locality. **B**. View of Kadmane Tea Estate with mountain range in southern Western Ghats, India.

Isometrus wayanadensis sp. nov.
urn:lsid:zoobank.org:act:2FC053B2-9202-4A22-8149-CBBE556C27AF
Figs 13–17, 18C, 19C, F, 21D, 23C, 25C; Table 3

Diagnosis (♂♀)

Total length 41.29–50.99 mm. Base colouration yellowish-brown and variegated with black-brown stripes and spots. Basal segments of chelicerae dorsally yellowish with blackish reticulation. Pectinal tooth number 15–18 in both sexes. Median supra-ocular region smooth. Median ocelli anteriorly situated in ratio of 1 : 2. Tergites I–VI sparsely and coarsely granular, with median carina stronger on posterior region. *Isometrus wayanadensis* sp. nov. differs from all other Indian species of *Isometrus* based on the following set of morphological characters:

1. Surface of carapace coarsely and densely granular (Figs 14C, 18C) as opposed to: coarsely and sparsely granular with some areas without granules in *I. sankeriensis* and *I. thurstoni*; finely and densely granular in *I. amboli*; granular throughout with mixed granules, more densely granular in inter-ocular area and median posterior ocular area in *I. kovariki*; and granular throughout but obsolete in *I. maculatus*.
2. Chela length to width ratio in males 5.0–5.3 as opposed to 6.1–6.5 in *I. tamhini*, 5.7–5.8 in *I. sankeriensis* and 10.6 in *I. nakshatra* sp. nov.; in females 4.7–5.0 as opposed to 5.2–5.9 in *I. tamhini*, 5.7 in *I. amboli*, and 6.1–6.2 in *I. nakshatra* sp. nov. (Tables 1–3).
3. Lateral patches on mesosomal tergites V and VI with fine granulation along margins (Fig. 21C) as opposed to coarse granulation along margins in *I. tamhini*.
4. Metasomal length to carapace length ratio in males 6.8–7.2 as opposed to 8.8–9.1 in *I. tamhini*, 5.9–6.1 in *I. sankeriensis*, 5.3–5.8 in *I. nakshatra* sp. nov., 7.6–8.2 in *I. thurstoni* and 9.6 in *I. maculatus* (Tables 1–3).
5. Lateral supramedian and ventral lateral carinae on metasomal segments II–IV moderately granular (Fig. 23C) as opposed to strongly granular in *I. tamhini* and *I. sankeriensis*.
6. Telson length to width ratio in males 3.9–4.2 as opposed to 4.6–4.8 in *I. tamhini* and 4.3 in *I. sankeriensis* (Tables 1–3).
7. Ventral median carina of telson vesicle moderately granular (Fig. 19F) as opposed to weakly granular in *I. sankeriensis*, *I. thurstoni*, *I. kovariki* and *I. nakshatra* sp. nov., and strongly granular in *I. tamhini*.
8. Spiniform granules of promedian carina of pedipalp patella strongly developed as opposed to moderately developed in *I. tamhini*, *I. amboli*, *I. sankeriensis* and *I. kovariki*, and weakly developed in *I. nakshatra* sp. nov. (Figs 24–25).

Etymology

The species epithet indicates the type locality of the new species, Wayanad National Park, in Kerala, India.

Material examined

Holotype

INDIA • ♂, adult; Kerala State, Wayanad District, Kidanganad; 11.70° N, 76.30° E; 929 m a.s.l.; 26 Dec. 2019; Shauri Sulakhe and Aditya Grover leg.; BNHS SC 190.

Paratypes

INDIA • 1 ♂, adult; same locality as for holotype; 1 Nov. 2020; Makarand Ketkar, Shubhankar Deshpande, Shauri Sulakhe and Swayam Thakkar leg.; INHER 279 • 3 ♀♀, adults; same locality as for holotype; 1 Nov. 2020; Makarand Ketkar, Shubhankar Deshpande, Shauri Sulakhe and Swayam Thakkar leg.; INHER 278, INHER 280, INHER 281 • 2 ♀♀, adults; same collection data as for preceding; BNHS

SC 191, BNHS SC 192 • 1 ♂, adult; Karnataka State, Kodagu District, K.S. Colony; 11.96° N, 76.05° E; 866 m a.s.l.; 1 Nov. 2020; Makarand Ketkar, Shubhankar Deshpande, Shauri Sulakhe and Swayam Thakkar leg.; BNHS SC 193.

Description (holotype, ♂, measurements in Table 3)

Colouration (Fig. 13A–B). Body and appendages yellowish and variegated with blackish brown stripes and spots; metasomal segment V dark brownish to blackish, darker on posterior portion; pedipalp fingers dark brownish. Ventral portion uniformly yellow and sternite VII with a few dark spots. Basal segments of chelicerae dorsally yellowish, with blackish reticulation ending anteriorly in a blackish transverse patch. Fingers of chelicerae dark brown with tip of fingers black. Telson reddish brown.

Carapace (Figs 14C, 18C). Surface coarsely and densely granular. Without carinae. Median supra-ocular area almost smooth on middle and posterior portion, distinctly granular on anterior portion. Inter-ocular area with coarse granules. Pair of median ocelli situated anteriorly, with median ocelli to anterior margin/median ocelli to posterior margin ratio of 1 : 2. Antero-lateral ocular tubercle granular, with type 5 lateral ocelli. Three pairs of large major ocelli and two small minor ocelli situated behind major ocelli. Longitudinal furrow moderately deep all along. Anterior margins smooth. Lateral margins weakly crenulated below lateral ocelli. Posterior margin almost entirely smooth.

Chelicerae (Fig. 13D). Characteristic of Buthidae. Basal segments and movable fingers with short, firm setae on basal and ventral surfaces.

Pedipalp (Figs 15, 25C). Femur with five carinae (prodorsal, retrodorsal, promedian, retromedian and proventral). All carinae crenulated. Intercarinal surfaces weakly granular except ventral surface smooth with a few fine granules on proximal portion. Patella with seven distinct carinae (dorsomedian, prodorsal, retrodorsal, retromedian, retroventral, promedian and proventral). Dorsal intercarinal surface weakly granular and ventral intercarinal surface smooth. Chela acarinate. Fixed fingers almost smooth. Movable and fixed fingers with six rows of prolateral and retrolateral denticles in pairs and single additional row of retrolateral denticles on proximal portion. Trichobothrial pattern typical for genus (chela dorsal 12, chela ventral 2, patella dorsal 6, patella retrolateral 7, femur dorsal 7 and femur prolateral 4).

Legs (Figs 13A–B, 14A–B). Femur and patellae carinated. All carinae granular. Tibiae 3 and 4 without tibial spurs. All legs with a pair of pedal spurs. Tarsomere covered with long delicate setae arranged in parallel rows on ventral side. Tarsomere I (basitarsus) with tuft of short, stout blackish setae on ventral side. Tarsomere II (telotarsus) compressed laterally and ventrally with paired row of short, pointed, anteriorly directed, closely placed setae.

Genital operculum (Fig. 13C). Wider than long, elliptical, separated, with a pair of short male genital papillae.

Pectines (Fig. 13C). Basal piece rectangular, deeply notched on anterior median margin. Posterior margin of basal piece curved. Marginal lamella of 3/3 digits and median lamella of 6/7 digits, outer margin armed with a row of stout, short red setae and a few setae on surface. Fulcra 15/15, roughly triangular, each armed with a few short red setae, placed in between adjacent pectinal teeth. Teeth 16/16, strong and stout.

Mesosoma (Figs 13A–B, 14A–B, 21C). Tergites I–VI sparsely and coarsely granular, with median carina more strongly developed on posterior side. Posterior and lateral margins granular. Lateral patches on mesosomal tergites V and VI with fine granulation along posterior margins. Tergite VII granular, narrowed posteriorly, with two pairs of lateral granular carinae. Broad median carina present, more strongly developed on anterior portion. Sternites III–VI almost entirely smooth, with a pair of spiracles. Sternite VII smooth on posterior margin, finely crenulated to serrated on lateral margins; two pairs of

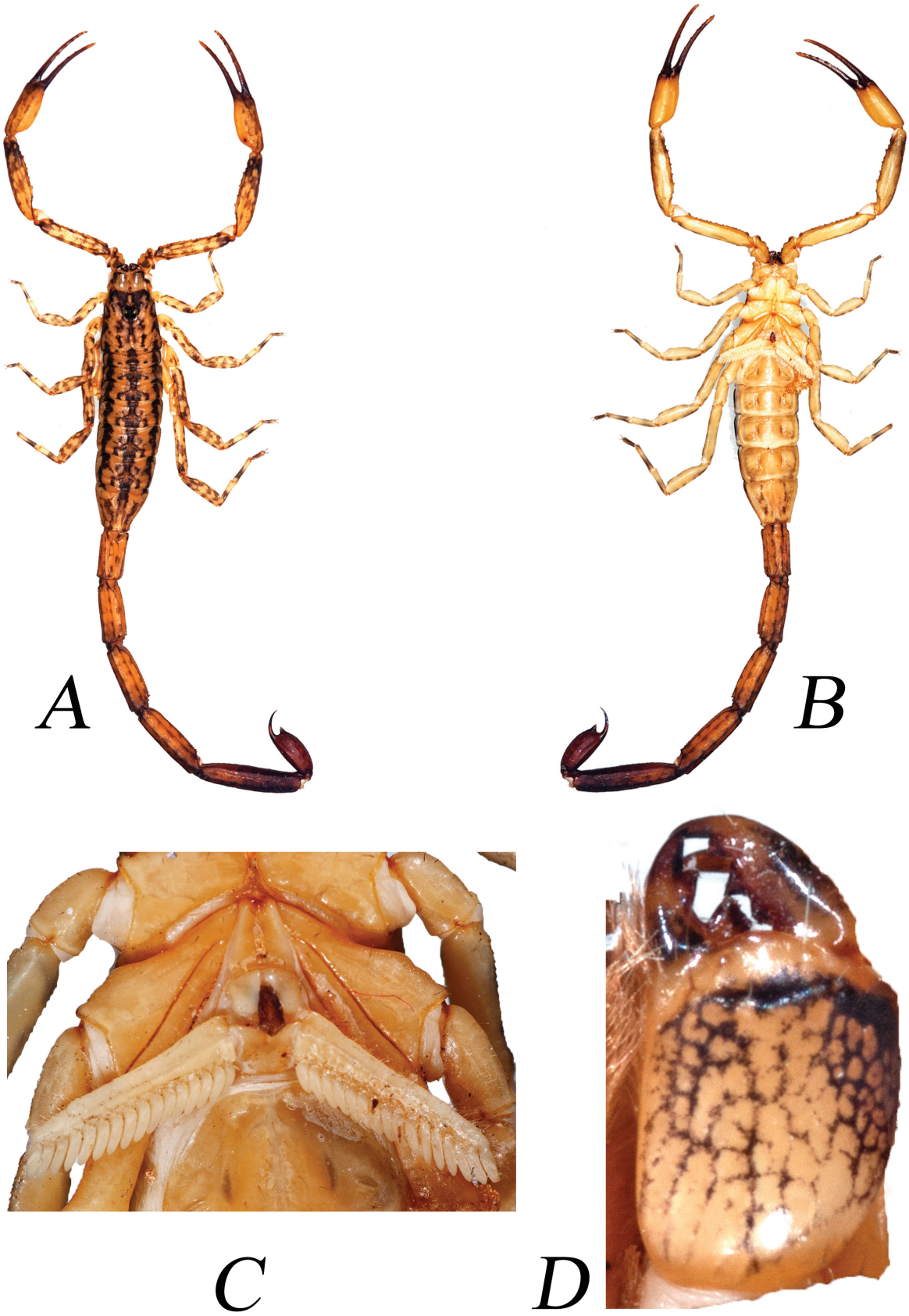

Fig. 13. *Isometrus wayanadensis* sp. nov., holotype, adult ♂ (BNHS SC 190). **A**. Dorsal view. **B**. Ventral view. **C**. Sternopectinal area. **D**. Chelicera, dorsal view.

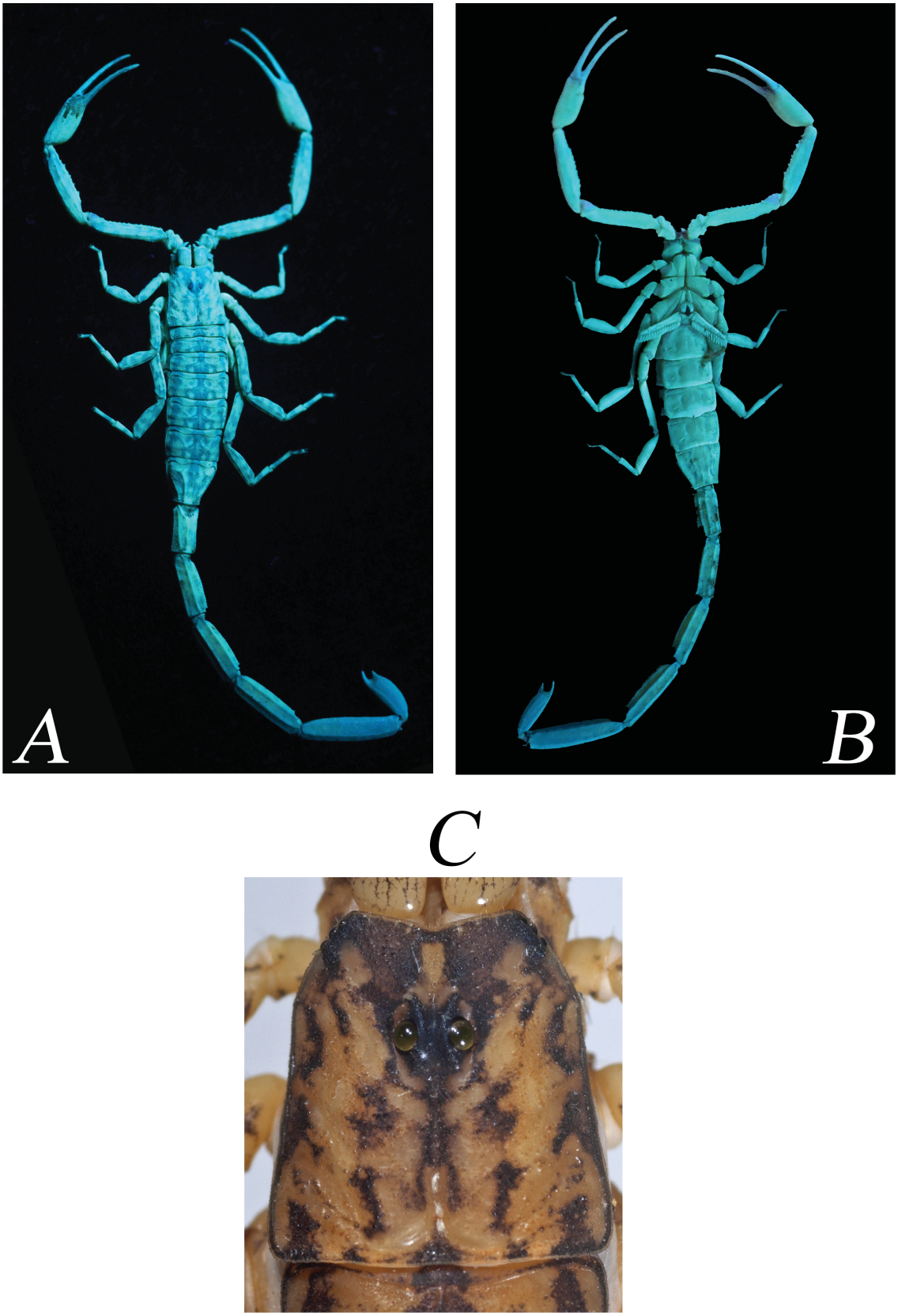

Fig. 14. *Isometrus wayanadensis* sp. nov., holotype, adult ♂ (BNHS SC 190). **A**. Dorsal view, UV light. **B**. Ventral view, UV light. **C**. Carapace, white light.

granular carinae with median carina present on posterior portion and lateral carina present along entrire length.

Metasoma (Figs 13A–B, 14A–B, 23C). All segments longer than wide. Segment I with five pairs of granular carinae (dorsal lateral, lateral supramedian, lateral inframedian, ventral lateral and ventral submedian). Intercarinal surfaces almost smooth. Segments II–IV with four pairs of carinae (dorsal lateral, lateral supramedian, ventral lateral and ventral submedian). Dorso-lateral and ventro-lateral carinae moderately granular. Lateral carina present on segment I only. Lateral supramedian and dorsal lateral carinae posteriorly ending in pointed, sub-triangular tubercles, more pointed on segments II and III. Intercarinal surfaces more granular on ventral portion. Segment V with five carinae (lateral supramedian pair, ventral lateral pair and single ventral median). Intercarinal surfaces finely granular. Anal rim almost smooth.

Telson (Fig. 19C, F). With elongated vesicle, smooth on dorsal surface. Ventral median carina moderately granular on distal portion, ending in triangular, subaculear, pointed nodule, armed with two pairs of minute denticles on inner margin. Ventral portion with two weak carinae. Lateral and ventral intercarinal surfaces weakly granular on distal portion only. Aculeus moderately elongated and sharp.

Distribution, habitat and ecology (Figs 17, 26)

Isometrus wayanadensis sp. nov. is known from the type locality, Kidanganad, Wayanad District, Kerala State, India, and one more locality, K.S. Colony, Kodagu District, Karnataka State, India, which is ca 60 km from the type locality. The new species is found under tree bark on tall trees in the moist deciduous and evergreen forest of Wayanad National Park (NP). A dense population of the new species was

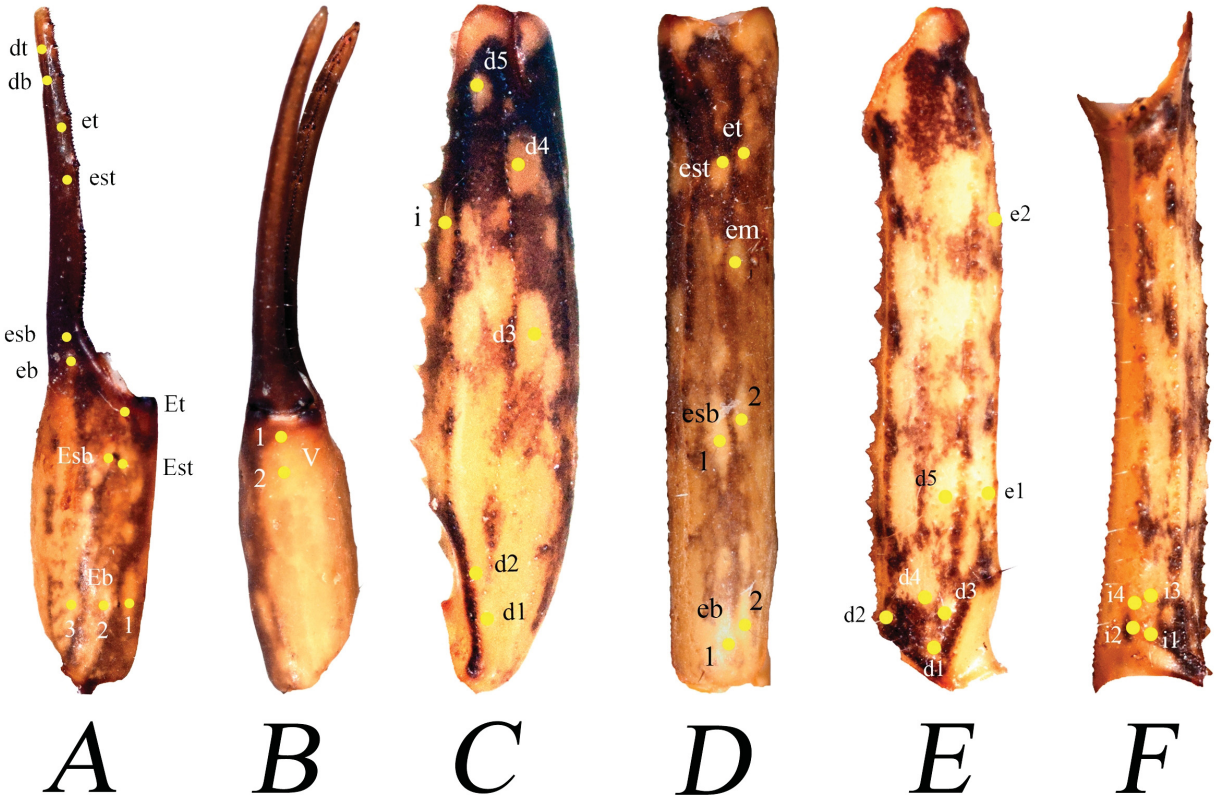

Fig. 15. *Isometrus wayanadensis* sp. nov., holotype, adult ♂ (BNHS SC 190). **A–B**. Pedipalp chela. **A**. Dorsal view. **B**. Ventral view. **C–D**. Patella. **C**. Dorsal view. **D**. External view. **E–F**. Femur. **E**. Dorsal view. **F**. Internal view. Trichobothrial pattern indicated by yellow dots.

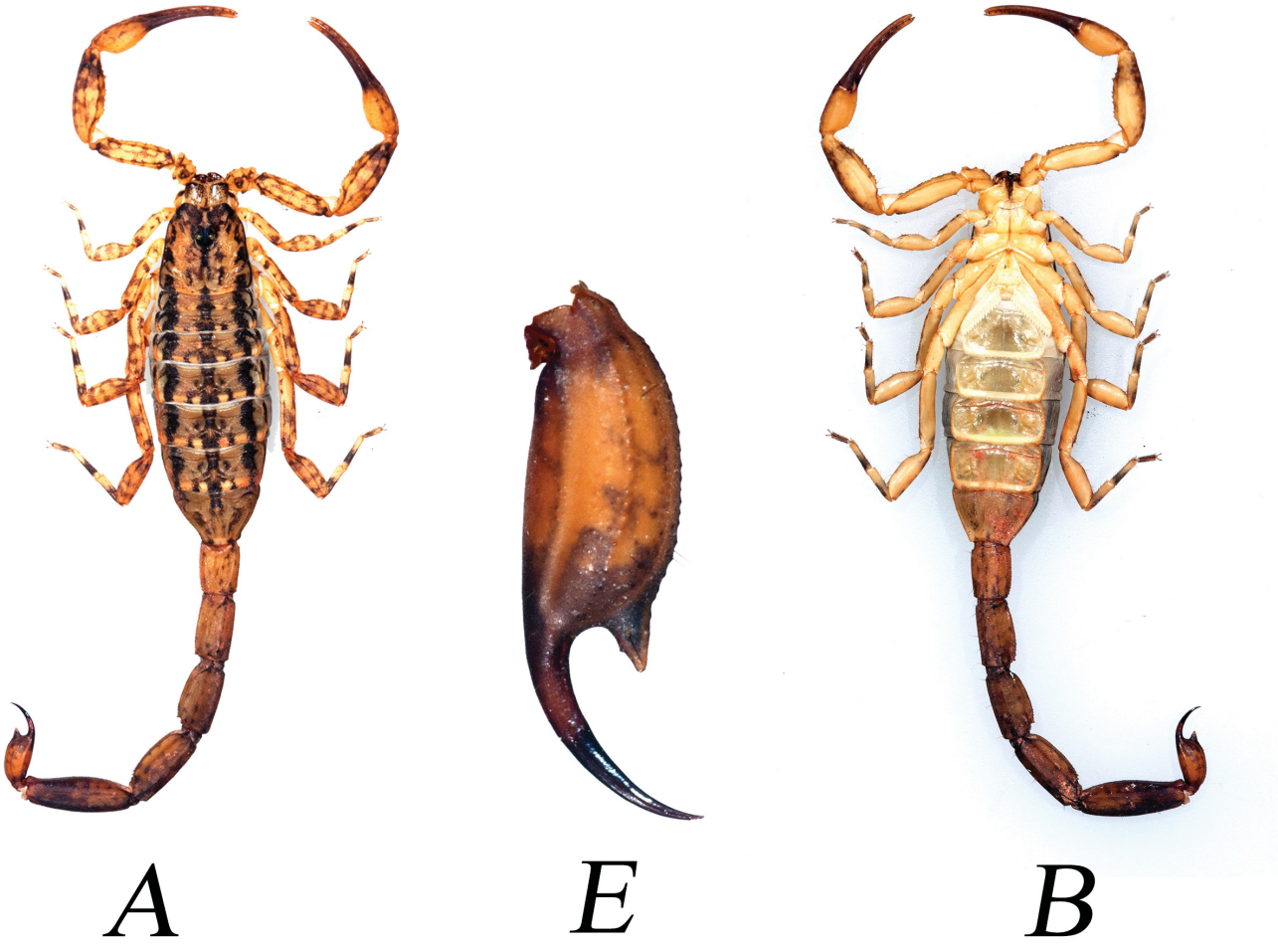

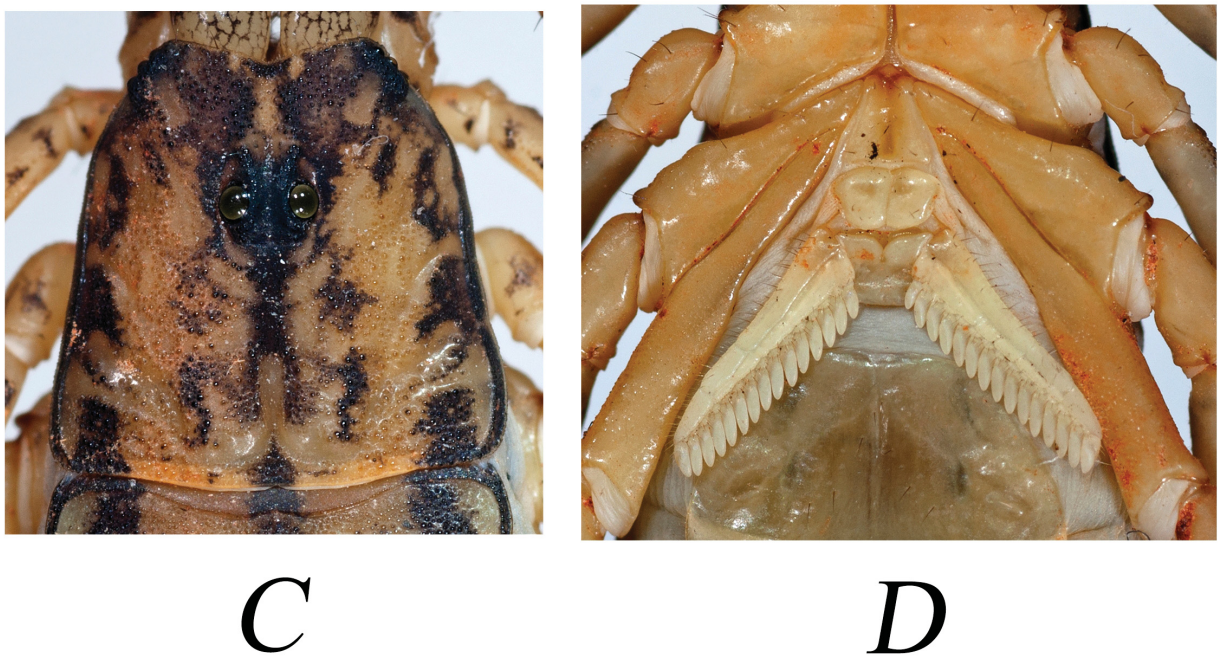

Fig. 16. *Isometrus wayanadensis* sp. nov., paratype, adult ♀ (BNHS SC 191). **A**. Dorsal view. **B**. Ventral view. **C**. Carapace, dorsal view. **D**. Sternopectinal area. **E**. Telson, lateral view.

Fig. 17. Type locality of *Isometrus wayanadensis* sp. nov. Views of tall evergreen forest along road at the type locality.

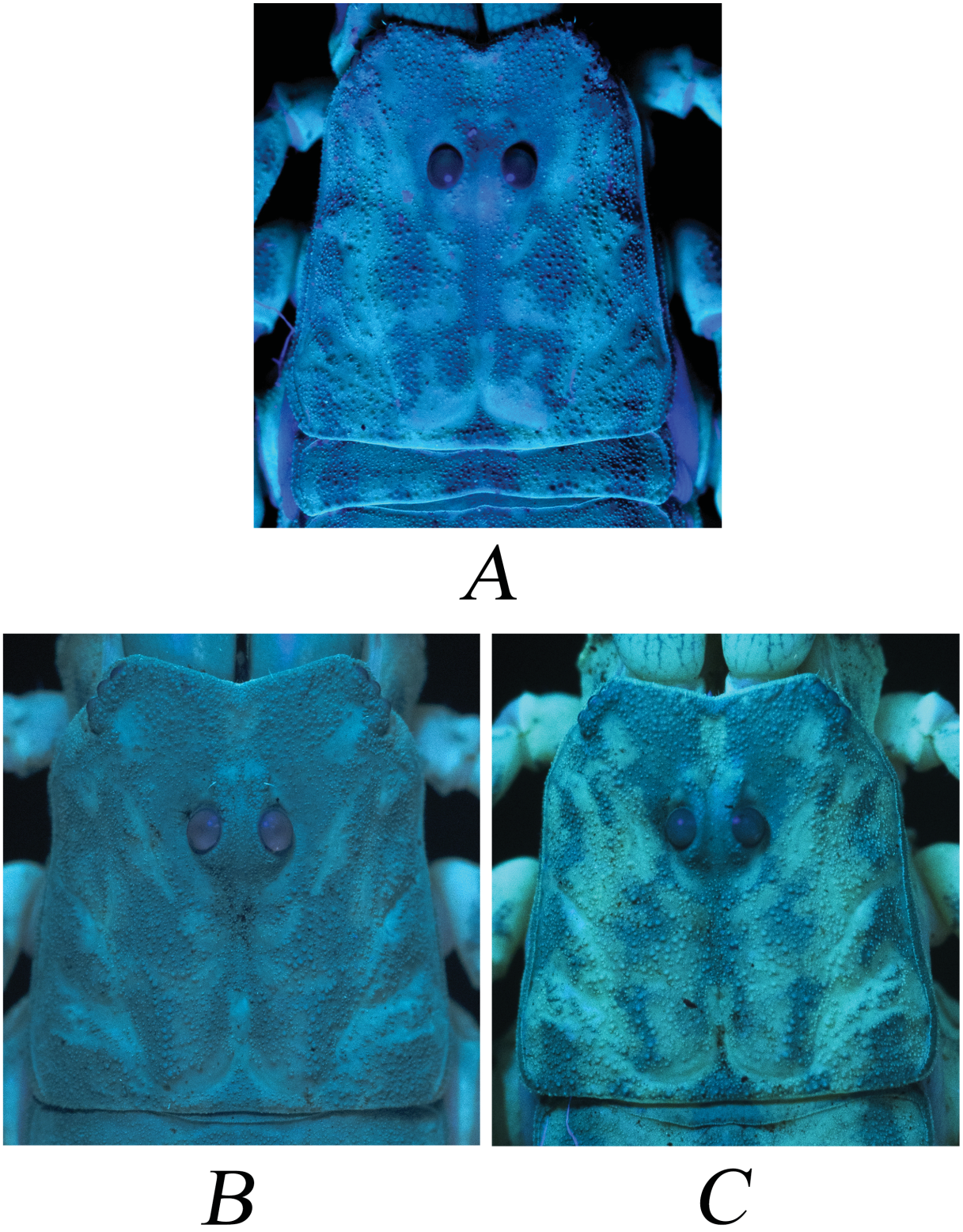

Fig. 18. Carapace under UV light. **A**. *Isometrus sankeriensis* Tikader & Bastawade, 1983, neotype, adult ♂ (BNHS SC 194). **B**. *I. nakshatra* sp. nov., holotype, adult ♂ (BNHS SC 195). **C**. *I. wayanadensis* sp. nov., holotype, adult ♂ (BNHS SC 190).

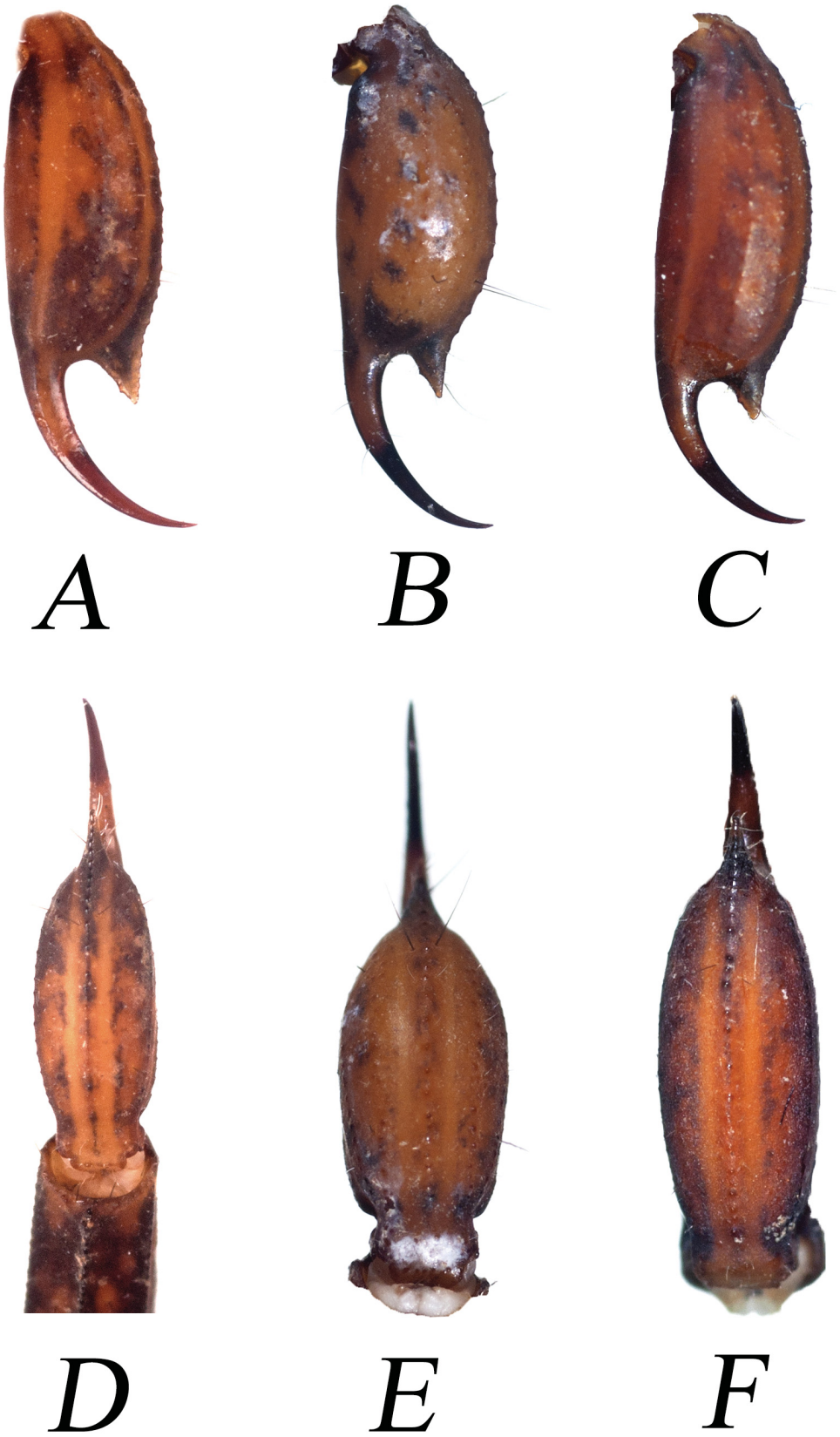

Fig. 19. A–**C**. Telson in lateral view. **D**–**F**. Telson in ventral view. **A, D**. *Isometrus sankeriensis* Tikader & Bastawade, 1983, neotype, adult ♂ (BNHS SC 194). **B, E**. *I. nakshatra* sp. nov., holotype, adult ♂ (BNHS SC 195). **C, F**. *I. wayanadensis* sp. nov., holotype, adult ♂ (BNHS SC 190).

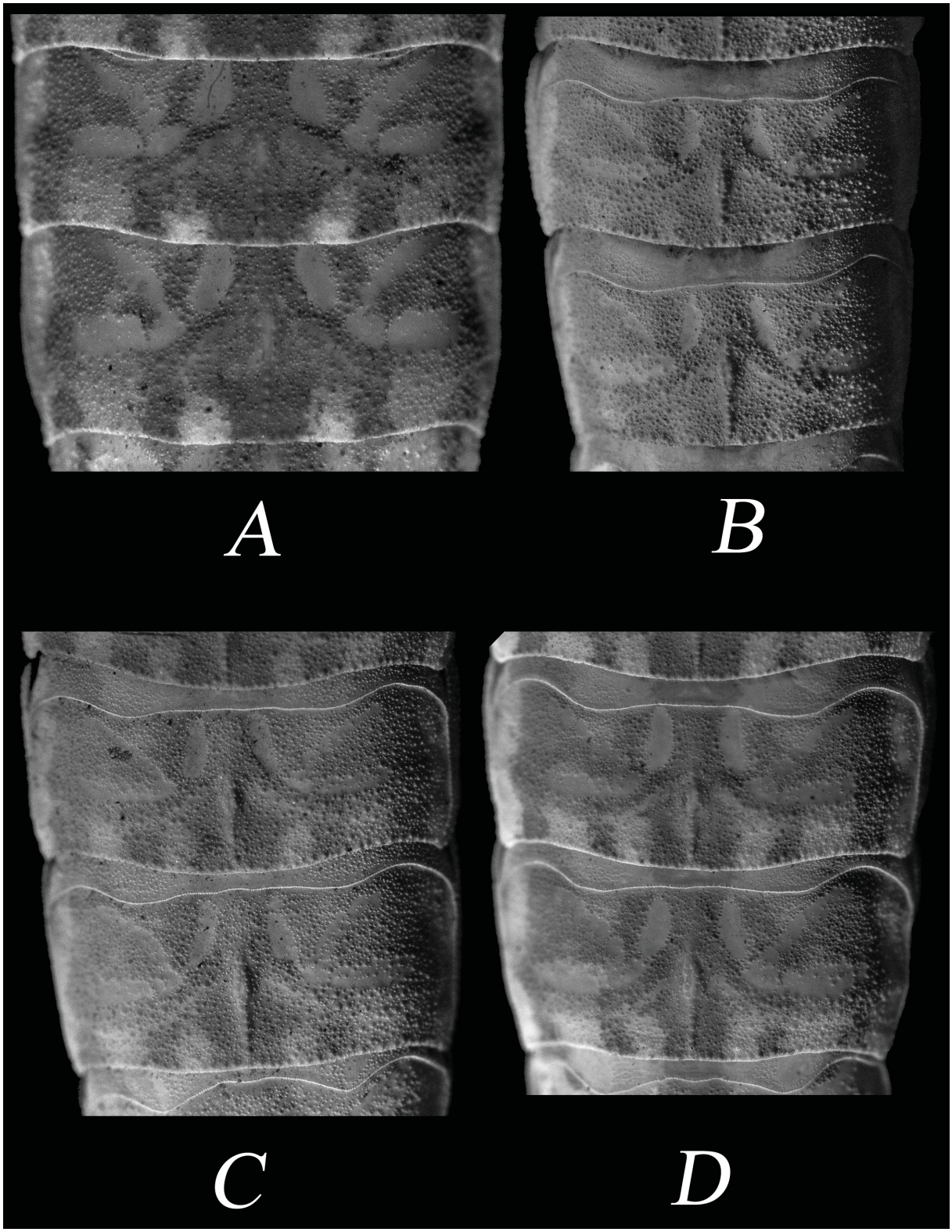

Fig. 20. Mesosomal tergites V and VI in dorsal view under UV light. **A**. *Isometrus thurstoni* Pocock, 1983, topotype, adult ♂ (INHER-139). **B**. *I. tamhini* Sulakhe *et al*., 2020, holotype, adult ♂ (BNHS SC 155). **C**. *I. amboli* Sulakhe *et al*., 2020, holotype, adult ♂ (BNHS SC 157). **D**. *I. kovariki* Sulakhe *et al*., 2020, holotype, adult ♂ (BNHS SC 161).

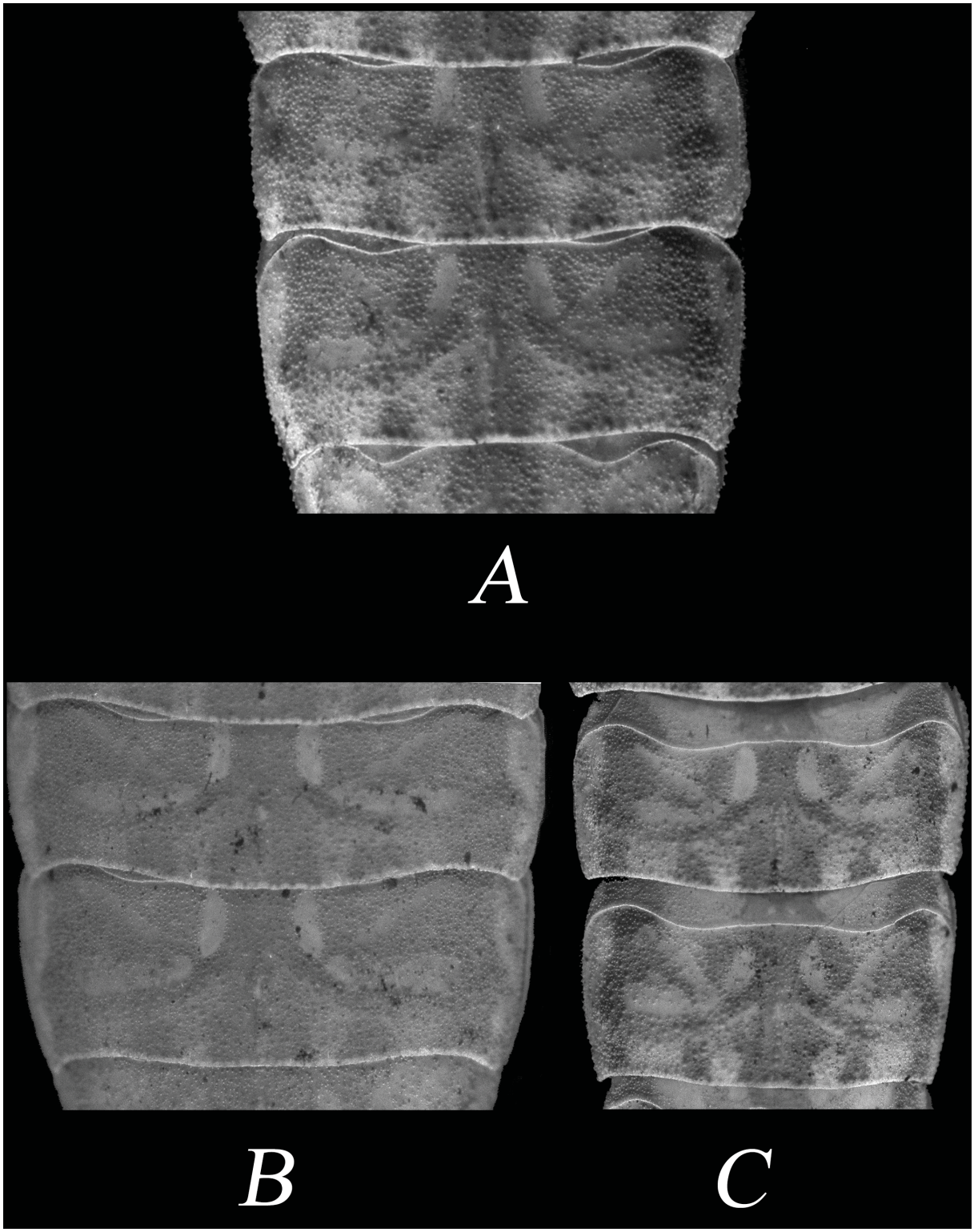

Fig. 21. Mesosomal tergites V and VI in dorsal view under UV light. **A**. *Isometrus sankeriensis* Tikader & Bastawade, 1983, neotype, adult ♂ (BNHS SC 194). **B**. *I. nakshatra* sp. nov., holotype, adult ♂ (BNHS SC 195). **C**. *I. wayanadensis* sp. nov., holotype, adult ♂ (BNHS SC 190).

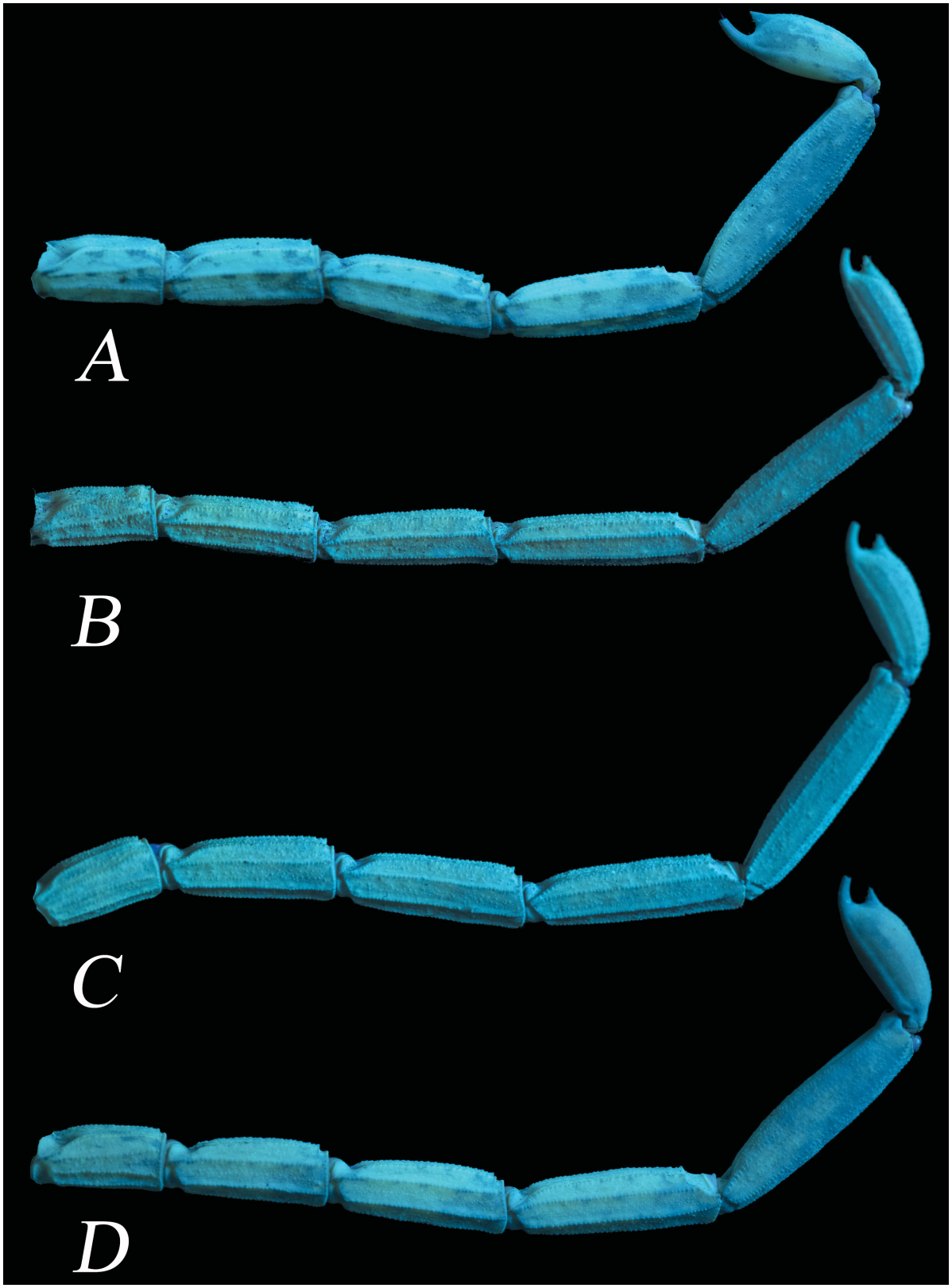

Fig. 22. Metasoma in lateral view under UV light. **A**. *Isometrus thurstoni* Pocock, 1983, topotype, adult ♂ (INHER 139). **B**. *I. tamhini* Sulakhe *et al*., 2020, holotype, adult ♂ (BNHS SC 155). **C**. *I. amboli* Sulakhe *et al*., 2020, holotype, adult ♂ (BNHS SC 157). **D**. *I. kovariki* Sulakhe *et al*., 2020, holotype, adult ♂ (BNHS SC 161).

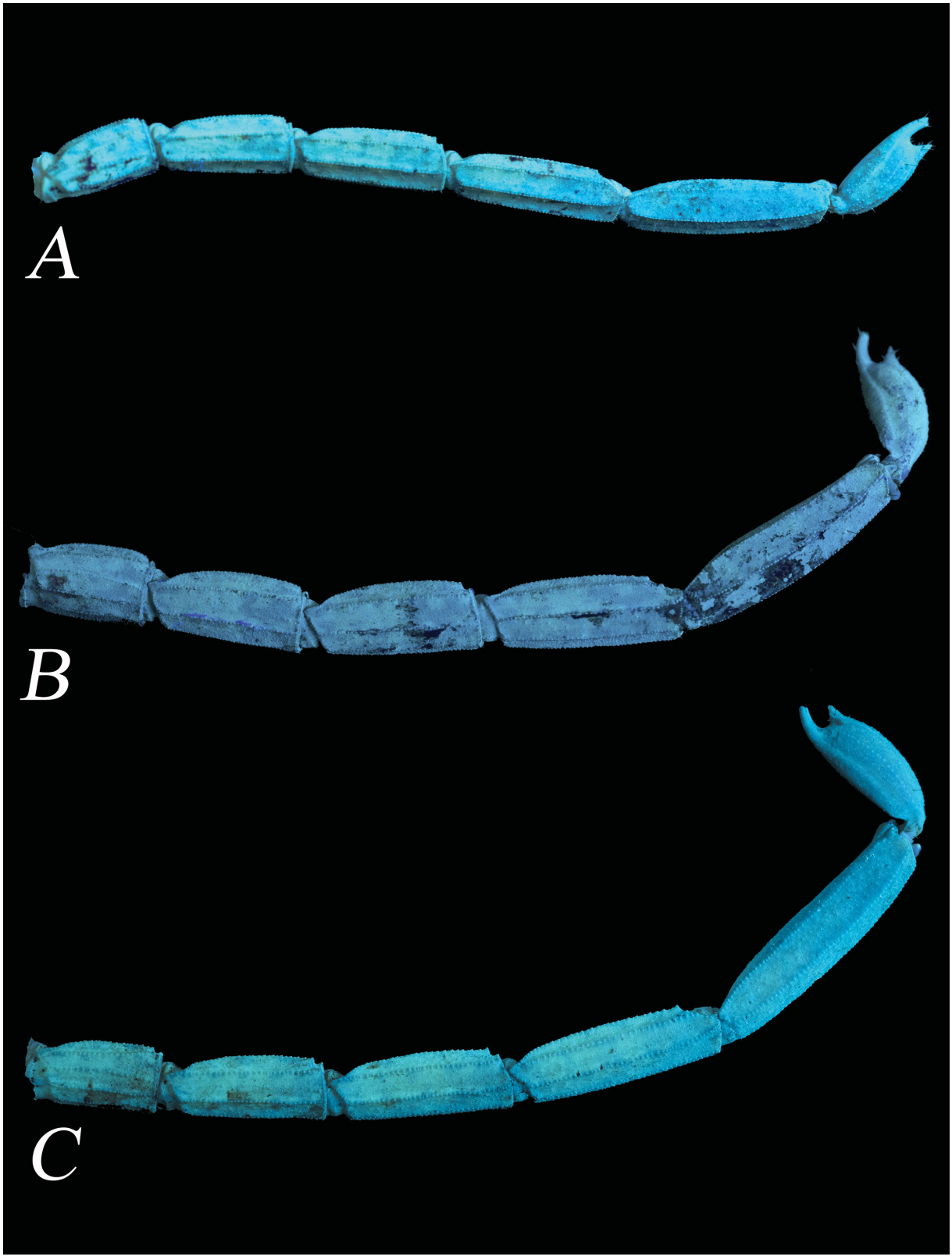

Fig. 23. Metasoma in lateral view under UV light. **A**. *Isometrus sankeriensis* Tikader & Bastawade, 1983, neotype, adult ♂ (BNHS SC 194). **B**. *I. nakshatra* sp. nov., holotype, adult ♂ (BNHS SC 195). **C**. *I. wayanadensis* sp. nov., holotype, adult ♂ (BNHS SC 190).

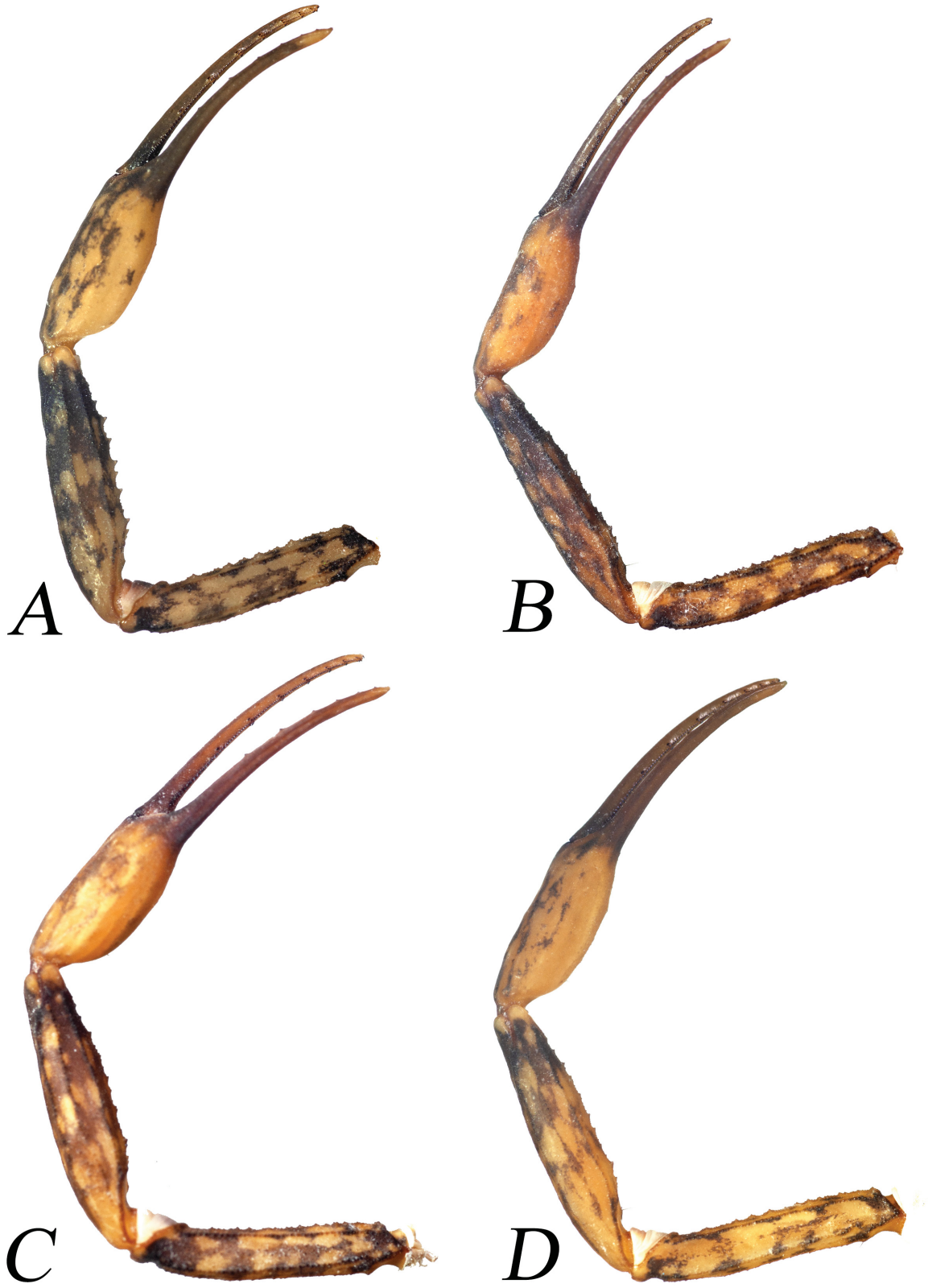

Fig. 24. Comparison of left pedipalps. **A**. *Isometrus thurstoni* Pocock, 1983, topotype, adult ♂ (INHER 139). **B**. *I. tamhini* Sulakhe *et al*., 2020, holotype, adult ♂ (BNHS SC 155). **C**. *I. amboli* Sulakhe *et al.,* 2020, holotype, adult ♂ (BNHS SC 157). **D**. *I. kovariki* Sulakhe *et al*., 2020, holotype, adult ♂ (BNHS SC 161).

Fig. 25. Comparison of left pedipalps. **A**. *Isometrus sankeriensis* Tikader & Bastawade, 1983, neotype, adult ♂ (BNHS SC 194). **B**. *I. nakshatra* sp. nov., holotype, adult ♂ (BNHS SC 195). **C**. *I. wayanadensis* sp. nov., holotype, adult ♂ (BNHS SC 190).

observed in the forest along the roads near the type locality. Wayanad NP is contiguous with Nagarhole NP, Bramhagiri Wildlife Sanctuary, and Bandipura NP and Tiger Reserve (TR) in Karnataka, and with Mudumalai NP and TR in Tamil Nadu, where the new species may occur in these protected areas; however, this needs to be confirmed with more sampling. The ecology of the new species is congruent with bark scorpions.

Key to Isometrus species from India

1. Ventral median carina on vesicle strongly granular .....***I. tamhini*** (Sulakhe *et al.*, 2020)
– Ventral median carina on vesicle moderately granular 2
– Ventral median carina on vesicle weakly granular 3

2. Surface of carapace coarsely and densely granular .....***I. wayanadensis*** sp. nov.
– Surface of carapace finely and densely granular .....***I. amboli*** (Sulakhe *et al.*, 2020)

3. Chela length to width ratio in males 10.6 .....***I. nakshatra*** sp. nov.
– Chela length to width ratio in males 5.0–6.4 4

4. Lateral supramedian and ventral lateral carinae on metasomal segments II–IV strongly granular; metasomal length to carapace length ratio in males 5.9–6.1 ....***I. sankeriensis*** (Tikader & Bastawade, 1983)
– Lateral supramedian and ventral lateral carinae on metasomal segments II–IV moderately to weakly granular; metasomal length to carapace length ratio in males 6.5–8.2 5

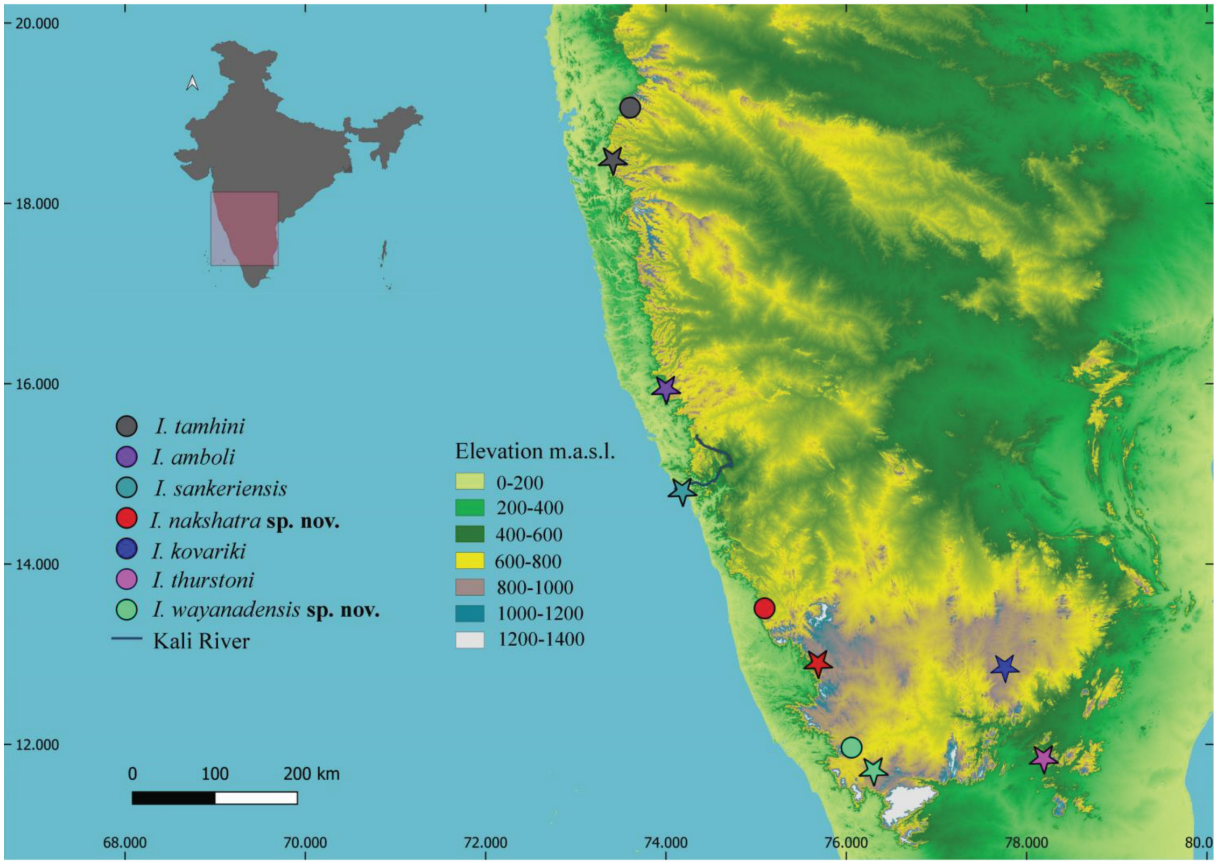

Fig. 26. Distribution of Indian species of *Isometrus* Ehrenberg, 1828 with elevation data. Stars represent type localities and circles represent additional sampled localities.

5. Surface of carapace coarsely and sparsely granular, with some areas without granules; anterior margin of carapace sharply curved near lateral ocelli .....***I. thurstoni*** (Pocock, 1983)
– Surface of carapace more closely granular in inter-ocular area and median posterior ocular area; anterior margin of carapace curved near lateral ocelli .....***I. kovariki*** (Sulakhe *et al.*, 2020)

Discussion

Our results confirm the high species diversity reported in recent studies on scorpions from India (Sulakhe *et al.* 2020a, 2020b, 2020c, 2020d, 2020e, 2021; Mirza 2020), highlighting the fact that scorpion diversity in India still remains underestimated. Discovering new species is not only important for understanding patterns of evolution, but also an important step towards prioritizing conservation needs and avoiding the risk of losing biodiversity even before it is taxonomically described.

The use of molecular phylogenetics has drastically improved our ability to understand speciation in scorpions. Reconstructing phylogenies using molecular data has become important, as some species may not show strong morphological differences, and thus integrative taxonomic approaches have gained rapid acceptance (Sulakhe *et al.* 2020a).

Isometrus sankeriensis and *I. amboli* look very similar, although the morphometric analysis show a clear difference between the two species and from all other Indian congeners. Sequences of *I. amboli* are closest to the sequences of *I. sankeriensis* and show a genetic divergence of 4.7–5.4% in *COI* and 2.6% in *16S*. However, these two species show a divergence from each other based on PTP and bPTP, GMYC, ABGD and share a TMRCA of 5 Mya. Low genetic distances among scorpion species have previously been reported in some buthid taxa (Fet *et al.* 2021). This low genetic divergence between some species of *Isomterus* from India may suggest recent speciation events between these species. *Isomterus sankeriensis* is also closely related to *I. tamhini* and sequences show a genetic divergence of 7.2–7.4% in *COI* and 4.2% in *16S*. There are also strong morphological characters distinguishing these two species. *Isometrus tamhini* can be clearly distinguished from all Indian congeners based on morphology. All sequences of *I. tamhini* are monophyletic in the *CO1* and *16S* concatenated gene tree and show closeness to *I. amboli* with a minimum genetic divergence of 6.6–7.2% in *COI* and 3.7% in *16S*. Sequences of *I. tamhini* (MT250512) from Saltar Khind (pass), near Telbaila Fort, Pune, ca 50 km from the type locality of *I. tamhini*, show a genetic divergence of 0.4% in the *COI* gene. Sequences of *I. tamhini* with the voucher numbers INHER 342 and INHER 343 from Bhimashanker, Pune, ca 100 km from the type locality of *I. tamhini*, show a genetic divergence of 0.6% in the *COI* gene. Locations from northern Western Ghats, such as Madheghat, Varandha Ghat (Pune), Harishchandragad (Ahmednagar), Mahabaleshwar and Jor-Jambhali (Satara), were surveyed extensively for populations of *Isometrus*, but no specimens were found.

Our integrated taxonomic approach with the time divergence data generated in this study has helped in understanding the cryptic diversity of *Isometrus* within the northern Western Ghats clade. Interestingly the River 'Kali' separates the populations of *I. sankeriensis* and *I. amboli*. Considering such a strong geographical barrier, it may not be possible to have a regular biotic interchange between these populations which may have led to a speciation event. Many such geographical barriers in Western Ghats would be the reason for genetic variation and speciation in *Isometrus.* Thus, more sampling from intervening locations across the Western Ghats-Sri Lanka biodiversity hotspot (Myers *et al.* 2000), with multi-gene phylogeny including nuclear genes, would not only help in attaining a better understanding of *Isometrus* diversity, but also throw light on the biogeography and evolutionary history of this group.

The use of internal morphological characters such as the hemispermatophore to identify species still remains understudied in Indian *Isometru*s. The ultimate goal of biodiversity conservation can be achieved by setting priorities, and the role of systematics is crucial in providing information for focused

conservation efforts (Bickford *et al.* 2007; McLeod 2010; Savage 1995). An accurate identification of species is essential to identifying regions with high levels of species richness and endemism. *Isometrus* has for many years been a genus with only two species known in India, having wide distributional ranges. It is now known to be a much more diverse genus with eight species found in India, all exhibiting restricted ranges and thus in urgent need of conservation.

Acknowledgements

We would like to thank Maharashtra Forest Department for granting the necessary permission for sample collection. We would like to thank InSearch Environmental Solutions for the institutional support and laboratory facilities. Shubhankar Deshpande is thankful to Hemant Karmarkar, Swati Athavale, Sunil Shilimkar, Chandrashekhar Ranjekar, Vishwanath Gosavi, Sachin Gosavi, Shrikant Abhyankar, Surendra Kulkarni, Varsha Agashe, Ravindra Joshi, Dhundiraj Gosavi, Sayali Ware, Priyanka Ahire, Madhuri Ganu, Shailaja Gore, Chaitali Hasbnis, Parag Atre, Jagannath Ahire, Mohini Gokhale, Jai Joshi and Neelam Adake for the crowd fund he received for this study. Shubhankar Deshpande is grateful to HoD (EVS) Fergusson College, Rupali Gaikwad for constant support and guidance. We are thankful to Deshabhushan Bastawade for his help in improving the manuscript. We are thankful to Pushkar Phansalkar, Swayam Thakkar and Amit Sayyed for their help during field work. We are thankful to Rahul Khot for his help during the registration of specimens at the Bombay Natural History Society (BNHS), Mumbai. We are thankful to Chaitanya Risbud for his help during the study of museum specimens and registration of specimens at the Institute of Natural History, Education and Research (INHER), Pune. We would also like to thank the anonymous reviewers for their constructive comments.

References

Altschul S.F., Gish W., Miller W., Myers E.W. & Lipman D.J. 1990. Basic local alignment search tool. *Journal of Molecular Biology* 215: 403–410.

Barrett R.D.H. & Hebert P.D.N. 2005. Identifying spiders through DNA barcodes. *Canadian Journal of Zoology* 83 (3): 481–491. https://doi.org/10.1139/z05-024

Bickford D., Lohman D.J., Sodhi N.S., Ng P.K.L., Meier R., Winker K., Ingram K.K. & Das I. 2007. Cryptic species as a window on diversity and conservation. *Trends in Ecology and Evolution* 22 (3): 148–155. https://doi.org/10.1016/j.tree.2006.11.004

Bossuyt F., Meegaskumbura M., Beenaerts N., Gower D.J., Pethiyagoda R., Roelants K., Mannaert A., Wilkinson M., Bahir M.M., Manamendra-Arachchi K., Ng P.K.L., Schneider C.J., Oommen O.V. & Milinkovitch M.C. 2004. Local endemism within the Western Ghats-Sri Lanka biodiversity hotspot. *Science* 306 (5695): 479–481. https://doi.org/10.1126/science.1100167

Buckingham K. & Weber S. 2016. *Assessing the ITTO Guidelines for the Restoration, Management and Rehabilitation of Degraded and Secondary Tropical Forests: Case Studies of Ghana, Indonesia and Mexico.* International Tropical Timber Organization, Yokohama, Japan.

Chaitanya R., Giri V.B., Deepak V., Datta-Roy A., Murthy B.H.C.K. & Karanth P. 2019. Diversification in the mountains: a generic reappraisal of the Western Ghats endemic gecko genus *Dravidogecko* Smith, 1933 (Squamata: Gekkonidae) with descriptions of six new species. *Zootaxa* 4688 (1): 1–56. https://doi.org/10.11646/zootaxa.4688.1.1

Doornik J.A. & Hansen H. 2008. An omnibus test for univariate and multivariate normality. *Oxford Bulletin of Economics and Statistics* 70 (Suppl. 1): 927–939. https://doi.org/10.1111/j.1468-0084.2008.00537.x

Edgar R.C. 2004. MUSCLE: multiple sequence alignment with high accuracy and high throughput. *Nucleic Acids Research* 32 (5): 1792–1797. https://doi.org/10.1093/nar/gkh340

Esposito L.A., Yamaguti H.Y., Pinto-da-Rocha R. & Prendini L. 2018. Plucking with the plectrum: phylogeny of the New World buthid scorpion subfamily Centruroidinae Kraus, 1955 (Scorpiones: Buthidae) reveals evolution of three pecten-sternite stridulation organs. *Arthropod Systematics and Phylogeny* 76 (1): 87–122.

Esselstyn J.A., Evans B.J., Sedlock J.L., Khan F.A.A. & Heaney L.R. 2012. Single-locus species delimitation: a test of the mixed yule-coalescent model, with an empirical application to Philippine round-leaf bats. *Proceedings of the Royal Society B: Biological Sciences* 279 (1743): 3678–3686. https://doi.org/10.1098/rspb.2012.0705

Fet V. & Lowe G. 2000. Family Buthidae C.L. Koch, 1837. *In*: Fet V., Sissom W.D., Lowe G. & Braunwalder M.E. (eds) *Catalog of the Scorpions of the World (1758–1998)*: 54–286. New York Entomological Society, New York.

Fet V., Kovařík F., Gantenbein B. & Graham M.R. 2021. Three new species of *Olivierus* (Scorpiones: Buthidae) from Kazakhstan and Uzbekistan. *Zootaxa* 5006 (1): 54–72. https://doi.org/10.11646/zootaxa.5006.1.9

Folmer O., Black M., Hoeh W., Lutz R. & Vrijenhoek R. 1994. DNA primers for amplification of mitochondrial cytochrome c oxidase subunit I from diverse metazoan invertebrates. *Molecular Marine Biology and Biotechnology* 3 (5): 294–299. https://doi.org/10.1071/ZO9660275

Francke O.F. 1977. Scorpions of the genus *Diplocentrus* from Oaxaca, Mexico (Scorpionida, Diplocentridae). *Journal of Arachnology* 4: 145–200.

Fujisawa T. & Barraclough T.G. 2013. Delimiting species using single-locus data and the generalized mixed yule coalescent approach: a revised method and evaluation on simulated data sets. *Systematic Biology* 62 (5): 707–724. https://doi.org/10.1093/sysbio/syt033

Giribet G., Carranza S., Baguñà J., Riutort M. & Ribera C. 1996. First molecular evidence for the existence of a Tardigrada+Arthropoda clade. *Molecular Biology and Evolution* 13 (1): 76–84. https://doi.org/10.1093/oxfordjournals.molbev.a025573

González-Santillán E. & Prendini L. 2013. Redefinition and generic revision of the North American vaejovid scorpion subfamily Syntropinae Kraepelin, 1905, with descriptions of six new genera. *Bulletin of the American Museum of Natural History* (382): 1–71. https://doi.org/10.1206/830.1

Gowande G., Pal S., Jablonski D., Masroor R., Phansalkar P.U., Dsouza P., Jayarajan A. & Shanker K. 2021. Molecular phylogenetics and taxonomic reassessment of the widespread agamid lizard *Calotes versicolor* (Daudin, 1802) (Squamata, Agamidae) across South Asia. *Vertebrate Zoology* 71: 669–696. https://doi.org/10.3897/vz.71.e62787

Hammer Ø., Harper D.A.T. & Ryan P.D. 2001. PAST: Paleontological statistics software package for education and data analysis. *Paleontologia Electronica* 4 (1): 9.

Hjelle J.T. 1990. Anatomy and morphology. *In*: Polis G.A. & Cloudsley-Thompson J. (eds) *The Biology of Scorpions*: 9–63. Stanford University Press, Stanford, CA, USA.

International Commission on Zoological Nomenclature 2000. *International Code of Zoological Nomenclature*. The International Trust for Zoological Nomenclature, London.

Kalyaanamoorthy S., Minh B.Q., Wong T.K.F., Von Haeseler A. & Jermiin L.S. 2017. ModelFinder: fast model selection for accurate phylogenetic estimates. *Nature Methods* 14 (6): 587–589. https://doi.org/10.1038/nmeth.4285

Kovařík F. 1994. *Isometrus zideki* sp. n. from Malaysia and Indonesia, and a taxonomic position of *I. formosus*, *I. thurstoni* and *I. sankeriensis* (Arachnida: Scorpionida: Buthidae). *Acta Societatis Zoologicae Bohemicae* 58: 195–203.

Kovařík F. 1997. *Isometrus* (*Reddyanus*) *kurkai* sp. n. from Indonesia (Scorpiones; Buthidae). *Časopis Národního Musea* 166 (1–4): 5–10.

Kovařík F. 2003. A review of the genus *Isometrus* Ehrenberg, 1828 (Scorpiones: Buthidae) with descriptions of four new species from Asia and Australia. *Euscorpius* 10: 1–19.

Kovařík F., Lowe G., Ranawana K.B., Hoferek D., Jayarathne V.S., Plíšková J. & Šťáhlavský F. 2016. Scorpions of Sri Lanka (Scorpiones: Buthidae, Chaerilidae, Scorpionidae) with description of four new species of the genera *Charmus* Karsch, 1879 and *Reddyanus* Vachon, 1972, stat. n. *Euscorpius* 220: 1–133.

Kumar S., Stecher G. & Tamura K. 2016. MEGA7: Molecular Evolutionary Genetics Analysis version 7.0 for bigger datasets. *Molecular Biology and Evolution* 33 (7): 1870–1874. https://doi.org/10.1093/molbev/msw054

Lajmi A., Giri V.B. & Karanth K.P. 2016. Molecular data in conjunction with morphology help resolve the *Hemidactylus brookii* complex (Squamata: Gekkonidae). *Organisms Diversity and Evolution* 16 (3): 659–677. https://doi.org/10.1007/s13127-016-0271-9

Lanfear R., Calcott B., Ho S.Y.W. & Guindon S. 2012. PartitionFinder: combined selection of partitioning schemes and substitution models for phylogenetic analyses. *Molecular Biology and Evolution* 29 (6): 1695–1701. https://doi.org/10.1093/molbev/mss020

Loria S.F. & Prendini L. 2014. Homology of the lateral eyes of scorpiones: a six-ocellus model. *PLoS One* 9 (12): e112913. https://doi.org/10.1371/journal.pone.0112913

Loria S.F. & Prendini L. 2020. Out of India, thrice: diversification of Asian forest scorpions reveals three colonizations of Southeast Asia. *Scientific Reports* 10 (1): 1–20. https://doi.org/10.1038/s41598-020-78183-8

Lourenço W.R. & Huber D. 2002. New addition to the scorpion fauna (Arachnida: Scorpiones) of Sri Lanka. *Revue suisse de Zoologie* 109 (2): 265–275. Available from https://www.biodiversitylibrary.org/page/41230145 [accessed 9 Mar. 2022].

Mallik A.K., Srikanthan A.N., Pal S.P., D'Souza P.M., Shanker K. & Ganesh S.R. 2020. Disentangling vines: a study of morphological crypsis and genetic divergence in vine snakes (Squamata: Colubridae: Ahaetulla) with the description of five new species from Peninsular India. *Zootaxa* 4874 (1): 1–62. https://doi.org/10.11646/zootaxa.4874.1.1

McLeod D.S. 2010. Of Least Concern? Systematics of a cryptic species complex: *Limnonectes kuhlii* (Amphibia: Anura: Dicroglossidae). *Molecular Phylogenetics and Evolution* 56 (3): 991–1000. https://doi.org/10.1016/j.ympev.2010.04.004

Minh B.Q., Schmidt H.A., Chernomor O., Schrempf D., Woodhams M.D., Von Haeseler A., Lanfear R. & Teeling E. 2020. IQ-TREE 2: New models and efficient methods for phylogenetic inference in the genomic era. *Molecular Biology and Evolution* 37 (5): 1530–1534. https://doi.org/10.1093/molbev/msaa015

Mirza Z.A. 2020. Two new species of buthid scorpion of the genus *Janalychas* Kovařík, 2019 (Arachnida: Scorpiones: Buthidae) from the Western Ghats, India. *Arachnology* 18 (4): 316–324. https://doi.org/10.13156/arac.2020.18.4.316

Mirza Z.A., Gowande G.G., Patil R., Ambekar M. & Patel H. 2018. First appearance deceives many: disentangling the *Hemidactylus triedrus* species complex using an integrated approach. *PeerJ* 6: e5341. https://doi.org/10.7717/peerj.5341

Mittermeier R.A., Robles Gil P., Hoffmann M., Pilgrim J., Brooks T., Mittermeier C.G., Lamoreux J. & da Fonseca G.A.B. 2004. *Hotspots Revisited: Earth's Biologically Richest and Most Endangered Ecoregions.* CEMEX, Mexico City.

Myers N., Mittermeier R.A., Mittermeier CG, Da Fonesca G.A. & Band Kent J. 2000. Biodiversity hotspots for conservation priorities. *Nature* 403: 853–858.

Nguyen L.T., Schmidt H.A., Von Haeseler A. & Minh B.Q. 2015. IQ-TREE: a fast and effective stochastic algorithm for estimating maximum-likelihood phylogenies. *Molecular Biology and Evolution* 32 (1): 268–274. https://doi.org/10.1093/molbev/msu300

Polis G.A., Sissom W.D. & McCormick S.J. 1981. Predators of scorpions: field data and a review. *Journal of Arid Environments* 4: 309–326. https://doi.org/10.1016/s0140-1963(18)31477-0

Prendini L. 2016. Redefinition and systematic revision of the East African scorpion genus *Pandinoides* (Scorpiones: Scorpionidae) with critique of the taxonomy of *Pandinus*, sensu lato. *Bulletin of the American Museum of Natural History* 407: 1–66. https://doi.org/10.1206/0003-0090-407.1.1

Prendini L., Crowe T.M. & Wheeler W.C. 2003. Systematics and biogeography of the family Scorpionidae (Chelicerata: Scorpiones), with discussion on phylogenetic methods. *Invertebrate Systematics* 17: 185–259.

Puillandre N., Lambert A., Brouillet S. & Achaz G. 2012. ABGD, Automatic Barcode Gap Discovery for primary species delimitation. *Molecular Ecology* 21 (8): 1864–1877. https://doi.org/10.1111/j.1365-294X.2011.05239.x

Rafinejad J., Shahi M., Navidpour S., Jahanifard E. & Hanafi-Bojd A.A. 2020. Effect of climate change on spatial distribution of scorpions of significant public health importance in Iran. *Asian Pacific Journal of Tropical Medicine* 13: 503–14.

Rambaut A. 2009. FigTree, ver 1.4.3. Available from http://tree.bio.ed.ac.uk/software/figtree [accessed 4 Mar. 2022].

Rambaut A., Drummond A.J., Xie D., Baele G. & Suchard M.A. 2018. Posterior summarization in Bayesian phylogenetics using Tracer 1.7. *Systematic Biology* 67 (5): 901–904. https://doi.org/10.1093/sysbio/syy032

Rein J.O. 2021. *The Scorpion Files.* Norwegian University of Science and Technology, Trondheim, Norway. Available from https://www.ntnu.no/ub/scorpion-files/ [accessed 19 Oct. 2021].

Savage J.M. 1995. Systematics and the biodiversity crisis. *Bioscience* 45 (10): 673–679.

Schwarz G. 1978. Estimating the dimension of a model. *Annals of Statistics* 6 (4): 461–464. https://doi.org/10.1214/aos/1176344136

Shanker K., Vijayakumar S.P. & Ganeshaiah K.N. 2017. Unpacking the species conundrum: philosophy, practice and a way forward. *Journal of Genetics* 96 (3): 413–430. https://doi.org/10.1007/s12041-017-0800-0

Simon C., Frati F., Beckenbach A., Crespi B., Liu H. & Flook P. 1994. Evolution, weighting, and phylogenetic utility of mitochondrial gene sequences and a compilation of conserved polymerase chain reaction primers. Annals of the Entomological Society of America 87 (6): 651–701. https://doi.org/10.1093/aesa/87.6.651

Stahnke H.L. 1970. Scorpion nomenclature and mensuration. *Entomological News* 81: 297–316. Available from https://www.biodiversitylibrary.org/page/2741128 [accessed 9 Mar. 2022].

Suchard M.A., Lemey P., Baele G., Ayres D.L., Drummond A.J. & Rambaut A. 2018. Bayesian phylogenetic and phylodynamic data integration using BEAST 1.10. *Virus Evolution* 4 (1): 1–5. https://doi.org/10.1093/ve/vey016

Sulakhe S., Dandekar N., Padhye A. & Bastawade D. 2020a. Two new cryptic species of *Isometrus* (Scorpiones: Buthidae) from India. *Euscorpius* 305: 1–24.

Sulakhe S., Dandekar N., Mukherjee S., Pandey M., Ketkar M., Padhye A. & Bastawade D. 2020b. A new species of *Isometrus* (Scorpiones: Buthidae) from southern India. *Euscorpius* 310: 1–13.

Sulakhe S., Sayyed Amit, Deshpande S., Dandekar N., Padhye A. & Bastawade D. 2020c. Taxonomic validity of *Neoscorpiops deccanensis*, *N. tenuicauda*, *N. satarensis* and *N. maharashtraensis* with description of a new species of *Neoscorpiops* Vachon, 1980 (Scorpiones: Euscorpiidae) from India. *Journal of the Bombay Natural History Society* 117: 1–21.

Sulakhe S., Deshpande S., Dandekar N., Ketkar M., Gowande G., Padhye A. & Bastawade D. 2020d. Two new species of *Chiromachetes* (Scorpiones: Hormuridae) from the northern Western Ghats, India. *Euscorpius* 320: 1–27.

Sulakhe S., Deshpande S., Dandekar N., Ketkar M., Padhye A. & Bastawade D. 2020e. A new cryptic species of *Scorpiops* Peters, 1861 (Scorpiones: Scorpiopidae) from the northern Western Ghats, India. *Euscorpius* 327: 1–18.

Sulakhe S., Deshpande S., Dandekar N., Padhye A. & Bastawade D. 2021. Four new lithophilic species of *Scorpiops* Peters, 1861 (Scorpiones: Scorpiopidae) from peninsular India. *Euscorpius* 337: 1–49.

Tawde S.A. & Singh C. 2015. Investigation of orographic features influencing spatial distribution of rainfall over the Western Ghats of India using satellite data. *International Journal of Climatology* 35 (9): 2280–2293. https://doi.org/10.1002/joc.4146

Tikader B.K. & Bastawade D.B. 1983. Scorpions (Scorpionida: Arachnida). Vol. III. *In*: Tikader B.K. (ed.) *The Fauna of India*. Zoological Survey of India, Calcutta [Kolkata].

Vachon M. 1974. Études des caractères utilisés pour classer les familles et les genres de scorpions (Arachnides). 1. La trichobothriotaxie en arachnologie. Sigles trichobothriaux et types de trichobothriotaxie chez les scorpions. *Bulletin du Muséum national d'Histoire naturelle, 3e Série* 140: 857–958.

Veronika K., Akilan K., Muruganathan A. & Eswaramohan T. 2013. Diversity and identification key to the species of scorpions (Scorpiones: Arachnida) from Jaffna Peninsula, Sri Lanka. *Jounal of Entomology and Zoology Studies* 1 (5): 70–77.

Zhang J., Kapli P., Pavlidis P. & Stamatakis A. 2013. A general species delimitation method with applications to phylogenetic placements. *Bioinformatics* 29 (22): 2869–2876. https://doi.org/10.1093/bioinformatics/btt499

Manuscript received: 30 October 2021
Manuscript accepted: 28 January 2022
Published on: 7 April 2022
Topic editor: Tony Robillard
Section editor: Rudy Jocqué
Desk editor: Danny Eibye-Jacobsen